established. Cumulative reports have shown that Th1/Tc1 type responses are instrumental in HCV-induced liver inflammation [7,25,26]. We thus hypothesized that some suppressor mechanisms exist in PNALT patients especially against HCV-specific Th1 and/or CTL reactions.

The involvement of Treg cells in the pathogenesis of various diseases has been reported [9–13]. Most of the studies presented the possibility that N-Treg play substantial roles in the induction of tolerance against aetiological self or nonself antigens, thus leading to alleviation or exacerbation of the disease severity. With regard to HCV infection, several groups have shown that N-Treg are increased both in the periphery and in the liver and are able to inhibit HCV-specific CD4+ or CD8+ T cell responses *in vitro* [17,18,27]. In this study, we showed that the frequency of N-Treg in HCV-infected patients is higher than those in the controls, which is consistent with the previous reports. However, the frequencies of N-Treg are indistinguishable between the patient groups with different disease activities. As for the functional aspect, the deprivation of CD4+CD25+ cells enhanced the HCV NS5-specific CD4+ T cell response in the PNALT than in the CH group, suggesting that co-existing Treg in the PNALT are more suppressive. In addition, the expression of FOXP3 and CTLA4, which are key molecules of the suppressor function, is higher in PNALT than in those with active hepatitis. Venken *et al.* [28] demonstrated that the degree of FOXP3 expression at the single-cell level of N-Treg is well correlated with their suppressive ability, which is supportive of our results. In contrast, Bolacchi *et al.* [29] reported that the frequency of TGF-β+ N-Treg in the PNALT was higher than in the hepatitis group. Furthermore, their frequency was inversely correlated with the histological inflammatory grade, suggesting that TGF-β+ Treg play active roles in alleviating hepatitis. The reasons for the lack of correlation between N-Treg and serum ALT or HCV RNA quantity in the present study may be because of the difference in the target of analyses, such as either peripheral or intra-hepatic Treg, or either TGF-β+ or bulk Treg. Further analyses need to be performed on these important issues, as CD4+FOXP3+ Treg are reported to accumulate more in the portal tract of HCV-infected livers compared with those in the periphery [20].

During the observation period, about 30–40% of PNALT patients began to show elevated or fluctuating ALT abnormalities. What crucial factor triggers HCV-induced liver inflammation remains unknown. One of the plausible explanations is an antigenic shift accompanied by the occurrence of mutations in the HCV genome. In other words, hepatitis may flare up if the mutation raises HCV immunogenicity. Comprehensive analyses of HCV epitopes for CTL using overlapping peptides have shown that the HCV core and NS3 are more immunogenic than the remaining regions; however, the presence of an epitope hierarchy in Treg induction has been controversial. Li *et al.* [30] reported the possibility that Treg are expandable in response to certain epitopes in HCV proteins. In two patients in whom we observed flare-up of hepatitis in this study, we were able to find that the expression of FOXP3 in N-Treg was high in the PNALT status, but declined in the active hepatitis stage (data not shown). Although it is difficult to state whether such phenotypic changes in N-Treg are the cause or the consequence of disease progression, these results suggest the involvement of N-Treg in the degree of HCV-mediated hepatitis. Further detailed study is needed to examine whether or not such changes in N-Treg are related to the sequence evolution in HCV genomes.

Recent research has disclosed that distinct types of Treg are present in humans. Currently, it is generally accepted that CD25+FOXP3+ is the most reliable marker for Treg, which is induced in parallel with the acquisition of suppressor ability. However, owing to the lack of phenotypic markers for specifically identifying adaptive Treg, their roles in clinical settings have been unclear. In this study, CD4+FOXP3+ cells increased in HCV-infected patients, who were either positive or negative for CD25. In contrast to thymus-derived N-Treg expressing a greater degree of CD25, adaptive Treg are presumed to be induced in the periphery with a lesser degree of CD25 expression. Thus, it is likely that CD4+CD25–FOXP3+ T cells in HCV infection contain some part of adaptive Treg.

Treg have been reported to express low levels of CD127 at their cell surface [31]. Furthermore, the expression of CD127 is inversely correlated with FOXP3 expression and with the suppressive function of CD25high+ Treg. Liu *et al.* [22] pointed out the possibility that adaptive Treg are grouped into CD127– cells, which also include FOXP3-negative Tr1 or Th3 cells. Alternatively, You *et al.* [32] reported that murine CD4+CD25lowFOXP3+ T cells might be adaptive Treg, which exert a TGFβ-dependent suppressive function. Taking these reports into consideration, and in order to exclude activated CD25+ T cells, we examined CD4+CD127–CD25–FOXP3+ cells tentatively determined as part of adaptive Treg. In order to confirm that CD4+CD127– cells possess suppressive capacity, we co-cultured sorted CD4+CD127–CD25– or CD4+CD127–CD25+ cells with allogeneic CD4+ T cells stimulated with anti-CD3 and anti-CD28 antibodies. As a result, we found that CD4+CD127– cells, regardless of CD25 expression, significantly suppressed the proliferation of responder CD4+ T cells (manuscript in preparation). Of note is the finding that the frequency of CD127–CD25–FOXP3+ cells is higher in patients with active hepatitis than those in the PNALT group. One of the plausible explanations for such an increase of Treg is the compensatory mechanisms for the aggravation of liver inflammation. In support of this possibility, Bonelli *et al.* [33] reported that CD4+CD127–CD25– cells are increased in patients with systemic lupus erythematosus (SLE), the numbers of which are well correlated with disease activity. With regard to the ability of Treg in SLE patients, CD4+CD127–CD25– cells were potent in the inhibition of T

cell proliferation but not in IFN-γ release. Such a defective suppressor capacity may result in the continuation of tissue inflammation regardless of the presence of abundant Treg. The other conceivable role of CD4+CD25–CD127–FOXP3+ cells in active hepatitis may be a peripheral reservoir of CD4+CD25+FOXP3+ cells in case of flare-up of liver inflammation. In mice, it has been reported that CD25–FOXP3+ cells revert to CD25+FOXP3+ cells upon activation signals, thus leading to the expansion of the Treg pool [34]. In order to reach a definite conclusion on the role of CD127–CD25–FOXP3+ cells, further analyses are needed to elucidate whether these cells are inhibitory to either HCV-specific or HCV-nonspecific T cell responses.

Large-scale studies with HCV-infected patients demonstrated that the cumulative incidence of HCC in the PNALT group is extremely low compared with that in patients with apparent hepatitis and liver cirrhosis [35]. The lesser HCC incidence is also evident in patients who attained a lasting biochemical response to IFN-based therapy; even if they had failed to achieve sustained virological response [36]. These results clearly indicate that the maintenance of the PNALT state is one of the surrogate therapeutic goals in chronic HCV infection. Therefore, it is necessary to clarify the mechanisms of Treg induction in HCV infection, whether they are naturally or adaptively introduced, and to establish a feasible modality for controlling Treg. Our study has shown the importance of subset-oriented analyses of Treg for gaining access to that goal.

ACKNOWLEDGEMENT

This study was funded in part by Ministry of Education, Culture, Sports, Science and Technology, Ministry of Health, Labor and Welfare of Japan.

CONFLICT OF INTEREST

All of the authors do not have any commercial or other association that might pose a conflict of interest.

REFERENCES

1 Kasahara A, Hayashi N, Mochizuki K *et al.* Risk factors for hepatocellular carcinoma and its incidence after interferon treatment in patients with chronic hepatitis C. Osaka Liver Disease Study Group. *Hepatology* 1998; 27(5): 1394–1402.
2 Marcellin P, Levy S, Erlinger S. Therapy of hepatitis C: patients with normal aminotransferase levels. *Hepatology* 1997; 26 (3 Suppl. 1): 133S–136S.
3 Tassopoulos NC. Treatment of patients with chronic hepatitis C and normal ALT levels. *J Hepatol* 1999; 31 (Suppl. 1): 193–196.
4 Persico M, Persico E, Suozzo R *et al.* Natural history of hepatitis C virus carriers with persistently normal aminotransferase levels. *Gastroenterology* 2000; 118(4): 760–764.
5 Suruki R, Hayashi K, Kusumoto K *et al.* Alanine aminotransferase level as a predictor of hepatitis C virus-associated hepatocellular carcinoma incidence in a community-based population in Japan. *Int J Cancer* 2006; 119(1): 192–195.
6 Nelson DR, Marousis CG, Davis GL *et al.* The role of hepatitis C virus-specific cytotoxic T lymphocytes in chronic hepatitis C. *J Immunol* 1997; 158(3): 1473–1481.
7 Schirren CA, Jung MC, Gerlach JT *et al.* Liver-derived hepatitis C virus (HCV)-specific CD4(+) T cells recognize multiple HCV epitopes and produce interferon gamma. *Hepatology* 2000; 32(3): 597–603.
8 Sakaguchi S. Naturally arising CD4+ regulatory T cells for immunologic self-tolerance and negative control of immune responses. *Annu Rev Immunol* 2004; 22: 531–562.
9 Viglietta V, Baecher-Allan C, Weiner HL, Hafler DA. Loss of functional suppression by CD4+CD25+ regulatory T cells in patients with multiple sclerosis. *J Exp Med* 2004; 199(7): 971–979.
10 Ehrenstein MR, Evans JG, Singh A *et al.* Compromised function of regulatory T cells in rheumatoid arthritis and reversal by anti-TNFalpha therapy. *J Exp Med* 2004; 200(3): 277–285.
11 Sugiyama H, Gyulai R, Toichi E *et al.* Dysfunctional blood and target tissue CD4+CD25high regulatory T cells in psoriasis: mechanism underlying unrestrained pathogenic effector T cell proliferation. *J Immunol* 2005; 174(1): 164–173.
12 Weiss L, Donkova-Petrini V, Caccavelli L, Balbo M, Carbonneil C, Levy Y. Human immunodeficiency virus-driven expansion of CD4+CD25+ regulatory T cells, which suppress HIV-specific CD4 T-cell responses in HIV-infected patients. *Blood* 2004; 104(10): 3249–3256.
13 Ormandy LA, Hillemann T, Wedemeyer H, Manns MP, Greten TF, Korangy F. Increased populations of regulatory T cells in peripheral blood of patients with hepatocellular carcinoma. *Cancer Res* 2005; 65(6): 2457–2464.
14 Jonuleit H, Schmitt E. The regulatory T cell family: distinct subsets and their interrelations. *J Immunol* 2003; 171(12): 6323–6327.
15 Hori S, Nomura T, Sakaguchi S. Control of regulatory T cell development by the transcription factor Foxp3. *Science* 2003; 299(5609): 1057–1061.
16 Fontenot JD, Rudensky AY. A well adapted regulatory contrivance: regulatory T cell development and the forkhead family transcription factor Foxp3. *Nat Immunol* 2005; 6(4): 331–337.
17 Cabrera R, Tu Z, Xu Y *et al.* An immunomodulatory role for CD4(+)CD25(+) regulatory T lymphocytes in hepatitis C virus infection. *Hepatology* 2004; 40(5): 1062–1071.
18 Rushbrook SM, Ward SM, Unitt E *et al.* Regulatory T cells suppress *in vitro* proliferation of virus-specific CD8+ T cells during persistent hepatitis C virus infection. *J Virol* 2005; 79(12): 7852–7859.
19 Sugimoto K, Ikeda F, Stadanlick J, Nunes FA, Alter HJ, Chang KM. Suppression of HCV-specific T cells without differential hierarchy demonstrated *ex vivo* in persistent HCV infection. *Hepatology* 2003; 38(6): 1437–1448.
20 Ward SM, Fox BC, Brown PJ *et al.* Quantification and localisation of FOXP3+ T lymphocytes and relation to

hepatic inflammation during chronic HCV infection. *J Hepatol* 2007; 47(3): 316–324.
21 Chen W, Jin W, Hardegen N *et al.* Conversion of peripheral CD4+CD25– naive T cells to CD4+CD25+ regulatory T cells by TGF-beta induction of transcription factor Foxp3. *J Exp Med* 2003; 198(12): 1875–1886.
22 Liu W, Putnam AL, Xu-Yu Z *et al.* CD127 expression inversely correlates with FoxP3 and suppressive function of human CD4+ Treg cells. *J Exp Med* 2006; 203(7): 1701–1711.
23 Kuzushita N, Hayashi N, Moribe T *et al.* Influence of HLA haplotypes on the clinical courses of individuals infected with hepatitis C virus. *Hepatology* 1998; 27(1): 240–244.
24 Kanto T, Inoue M, Miyazaki M *et al.* Impaired function of dendritic cells circulating in patients infected with hepatitis C virus who have persistently normal alanine aminotransferase levels. *Intervirology* 2006; 49(1–2): 58–63.
25 Leroy V, Vigan I, Mosnier JF *et al.* Phenotypic and functional characterization of intrahepatic T lymphocytes during chronic hepatitis C. *Hepatology* 2003; 38(4): 829–841.
26 Penna A, Missale G, Lamonaca V *et al.* Intrahepatic and circulating HLA class II-restricted, hepatitis C virus-specific T cells: functional characterization in patients with chronic hepatitis C. *Hepatology* 2002; 35(5): 1225–1236.
27 Boettler T, Spangenberg HC, Neumann-Haefelin C *et al.* T cells with a CD4+CD25+ regulatory phenotype suppress *in vitro* proliferation of virus-specific CD8+ T cells during chronic hepatitis C virus infection. *J Virol* 2005; 79(12): 7860–7867.
28 Venken K, Hellings N, Thewissen M *et al.* Compromised CD4+ CD25(high) regulatory T-cell function in patients with relapsing-remitting multiple sclerosis is correlated with a reduced frequency of FOXP3-positive cells and reduced FOXP3 expression at the single-cell level. *Immunology* 2008; 123(1): 79–89.
29 Bolacchi F, Sinistro A, Ciaprini C *et al.* Increased hepatitis C virus (HCV)-specific CD4+CD25+ regulatory T lymphocytes and reduced HCV-specific CD4+ T cell response in HCV-infected patients with normal versus abnormal alanine aminotransferase levels. *Clin Exp Immunol* 2006; 144(2): 188–196.
30 Li S, Jones KL, Woollard DJ *et al.* Defining target antigens for CD25+ FOXP3+ IFN-gamma-regulatory T cells in chronic hepatitis C virus infection. *Immunol Cell Biol* 2007; 85(3): 197–204.
31 Seddiki N, Santner-Nanan B, Martinson J *et al.* Expression of interleukin (IL)-2 and IL-7 receptors discriminates between human regulatory and activated T cells. *J Exp Med* 2006; 203(7): 1693–1700.
32 You S, Leforban B, Garcia C, Bach JF, Bluestone JA, Chatenoud L. Adaptive TGF-beta-dependent regulatory T cells control autoimmune diabetes and are a privileged target of anti-CD3 antibody treatment. *Proc Natl Acad Sci USA* 2007; 104(15): 6335–6340.
33 Bonelli M, Savitskaya A, Steiner CW, Rath E, Smolen JS, Scheinecker C. Phenotypic and functional analysis of CD4+CD25– Foxp3+ T cells in patients with systemic lupus erythematosus. *J Immunol* 2009; 182(3): 1689–1695.
34 Zelenay S, Lopes-Carvalho T, Caramalho I, Moraes-Fontes MF, Rebelo M, Demengeot J. Foxp3+ CD25– CD4 T cells constitute a reservoir of committed regulatory cells that regain CD25 expression upon homeostatic expansion. *Proc Natl Acad Sci USA* 2005; 102(11): 4091–4096.
35 Okanoue T, Makiyama A, Nakayama M *et al.* A follow-up study to determine the value of liver biopsy and need for antiviral therapy for hepatitis C virus carriers with persistently normal serum aminotransferase. *J Hepatol* 2005; 43(4): 599–605.
36 Tanaka H, Tsukuma H, Kasahara A *et al.* Effect of interferon therapy on the incidence of hepatocellular carcinoma and mortality of patients with chronic hepatitis C: a retrospective cohort study of 738 patients. *Int J Cancer* 2000; 87(5): 741–749.

Journal of Viral Hepatitis, 2009, 16, 578–585 doi:10.1111/j.1365-2893.2009.01116.x

Pegylated interferon alpha-2b (Peg-IFN α-2b) affects early virologic response dose-dependently in patients with chronic hepatitis C genotype 1 during treatment with Peg-IFN α-2b plus ribavirin

T. Oze,[1,*] N. Hiramatsu,[1,*] T. Yakushijin,[1] M. Kurokawa,[1] T. Igura,[1] K. Mochizuki,[1] K. Imanaka,[2] A. Yamada,[3] M. Oshita,[4] H. Hagiwara,[5] E. Mita,[6] T. Ito,[7] Y. Inui,[8] T. Hijioka,[9] S. Tamura,[10] H. Yoshihara,[11] E. Hayashi,[12] A. Inoue,[13] Y. Imai,[14] M. Kato,[15] Y. Yoshida,[1] T. Tatsumi,[1] K. Ohkawa,[1] S. Kiso,[1] T. Kanto,[1] A. Kasahara,[1] T. Takehara[1] and N. Hayashi[1]

[1]*Department of Gastroenterology and Hepatology, Osaka University Graduate School of Medicine, Yamadaoka, Suita, Osaka, Japan;* [2]*Osaka Medical Center for Cancer and Cardiovascular Diseases, Osaka, Osaka, Japan;* [3]*Sumitomo Hospital, Osaka, Osaka, Japan;* [4]*Osaka Police Hospital, Osaka, Osaka, Japan;* [5]*Higashiosaka City Central Hospital, Higashiosaka, Osaka, Japan;* [6]*National Hospital Organization Osaka National Hospital, Osaka, Osaka, Japan;* [7]*Kansai Rousai Hospital, Amagasaki, Hyogo, Japan;* [8]*Hyogo Prefectural Nishinomiya Hospital, Nishinomiya, Hyogo, Japan;* [9]*National Hospital Organization Osaka Minami Medical Center, Kawachinagano, Osaka, Japan;* [10]*Minoh City Hospital, Minoh, Osaka, Japan;* [11]*Osaka Rousai Hospital, Sakai, Osaka, Japan;* [12]*Kinki Central Hospital of Mutual Aid Association of Public School Teachers, Itami, Hyogo, Japan;* [13]*Osaka General Medical Center, Osaka, Osaka, Japan;* [14]*Ikeda Municipal Hospital, Ikeda, Osaka, Japan; and* [15]*National Hospital Organization Minami Wakayama Medical Center, Tanabe, Wakayama, Japan*

Received November 2008; accepted for publication December 2008

SUMMARY. Chronic hepatitis C (CH-C) genotype 1 patients who achieved early virologic response have a high probability of sustained virologic response (SVR) following pegylated interferon (Peg-IFN) plus ribavirin therapy. This study was conducted to evaluate how reducing drug doses affects complete early virologic response (c-EVR) defined as hepatitis C virus (HCV) RNA negativity at week 12. Nine hundred eighty-four patients with CH-C genotype 1 were enrolled. Drug doses were evaluated independently on a body weight base from doses actually taken. From multivariate analysis, the mean dose of Peg-IFN α-2b during the first 12 weeks was the independent factor for c-EVR ($P = 0.02$), not ribavirin. The c-EVR rate was 55% in patients receiving ≥1.2 μg/kg/week of Peg-IFN, and declined to 38% at 0.9–1.2 μg/kg/week, and 22% in patients given <0.9 μg/kg/week ($P < 0.0001$). Even with stratified analysis according to ribavirin dose, the dose-dependent effect of Peg-IFN on c-EVR was observed, and similar c-EVR rates were obtained if the dose categories of Peg-IFN were the same. Furthermore, the mean dose of Peg-IFN during the first 12 weeks affected HCV RNA negativity at week 24 ($P < 0.0001$) and SVR ($P < 0.0001$) in a dose-dependent manner. Our results suggest that Peg-IFN was dose-dependently correlated with c-EVR, independently of ribavirin dose. Thus, maintaining the Peg-IFN dose as high as possible during the first 12 weeks can yield HCV RNA negativity and higher c-EVR rates, leading to better SVR rates in patients with CH-C genotype 1.

Keywords: chronic hepatitis C, drug dose, early virologic response, HCV RNA negativity, pegylated interferon plus ribavirin, sustained virologic response.

INTRODUCTION

Pegylated interferon (Peg-IFN) plus ribavirin therapy can improve anti-viral efficacy for patients with chronic hepatitis C [1–5], and the prognosis of patients in whom hepatitis C virus (HCV) is successfully eradicated improves markedly [6–10]. However, HCV still persists in approximately half of genotype 1 patients treated with Peg-IFN plus ribavirin [2–4]. Therefore, the treatment method needs to be well managed in order to maximize the virologic response in these patients with HCV genotype 1.

Abbreviations: c-EVR, complete EVR; CH-C, chronic hepatitis C; EVR, early virologic response; G-CSF, granulocyte-macrophage colony stimulating factor; Hb, haemoglobin; HCV, hepatitis C virus; Peg-IFN, pegylated interferon; Plt, platelet; SVR, sustained virologic response; WBC, white blood cell.

Correspondence: Naoki Hiramatsu, MD, PhD, Department of Gastroenterology and Hepatology, Osaka University Graduate School of Medicine, 2-2, Yamadaoka, Suita City, Osaka 565-0871, Japan. E-mail hiramatsu@gh.med.osaka-u.ac.jp

*These authors contributed equally to this work.

In order to achieve sustained virologic response (SVR), earlier virologic response is very important for patients with chronic hepatitis C (CH-C) genotype 1. A high SVR rate (65–72%) was found in patients who achieved early virologic response (EVR) defined as a 2-log decrease in HCV RNA level at week 12, but only 0–3% SVR was seen in patients without EVR [3,11]. Additionally, complete EVR (c-EVR), which means HCV RNA negativity at week 12, is more strongly related to SVR [3].

The relationship between drug exposure and anti-viral effect has been reported in several papers [2,11–15]. McHutchison *et al.* [12] demonstrated that the SVR rate in patients who received ≥80% of their total planned doses of Peg-IFN and ribavirin for ≥80% of the scheduled duration of therapy was significantly higher than that of patients who received <80% of one or both drugs (51% *vs* 34%) and also suggested that the impact of dose reduction was greatest in patients for whom the dose had to be decreased within the first 12 weeks of treatment. In a subsequent analysis, reducing the dose of Peg-IFN and ribavirin to <80% of the full planned dose within the first 12 weeks was reported to reduce EVR rate from 80 to 33% [11]. Thus, drug adherence during the first 12 weeks has been shown to be very important for attaining EVR and SVR, but it remains obscure whether either drug can be reduced to a certain degree without adversely affecting the treatment efficacy.

In the present study, we examined the correlation between c-EVR and drug doses which are evaluated on a body weight basis from drug doses actually taken, in order to clarify the necessary drug exposure of Peg-IFN and ribavirin for achieving a higher c-EVR rate in patients with CH-C genotype 1.

PATIENTS AND METHODS

Patients

The current study was a retrospective, multicenter trial conducted by Osaka University Hospital and other institutions participating in the Osaka Liver Forum. A total of 984 patients with CH-C treated with a combination of Peg-IFN α-2b plus ribavirin were enrolled in this study between December 2004 and September 2006. The baseline characteristics of the patients are summarized in Table 1. All patients were Japanese, their mean age was 56.3 ± 10.1 years, and 56% were males. The mean serum alanine aminotransferase level was 79 ± 61 IU/L.

Patients eligible for this study were those who were infected with HCV genotype 1 and had a viral load of more than 10^5 IU/mL, but were negative for hepatitis B surface antigen or anti-human immunodeficiency virus. Patients were excluded from this study if they had decompensated cirrhosis or other forms of liver disease (alcohol liver disease, autoimmune hepatitis). Informed consent was obtained from each patient included in this study. This study was conducted according to the ethical guidelines of the 1975 Declaration of Helsinki and informed consent was obtained from each patient.

Table 1 Baseline characteristics of patients

Factor	Mean ± SD or number
n	984
Age (year)	56.3 ± 10.1
Sex: male/female	555/429
Body weight (kg)	61.8 ± 11.5
History of interferon treatment	
Naïve/experienced (relapser/nonresponder)*	575/409(160/182)
White blood cells (per mm^3)	5052 ± 1550
Neutrophils (per mm^3)	2577 ± 1092
Red blood cells ($\times 10^4/mm^3$)	442 ± 47
Haemoglobin (g/dL)	14.1 ± 1.4
Platelets ($\times 10^4/mm^3$)	15.9 ± 5.5
AST (IU/L)	66 ± 45
ALT (IU/L)	79 ± 61
Serum HCV RNA (kIU/mL)†	1600
Histology (METAVIR)‡	
Fibrosis; 0/1/2/3/4	49/314/197/105/18
Activity; 0/1/2/3	23/329/304/27

AST, aspartate aminotransferase; ALT, alanine aminotransferase; HCV, hepatitis C virus.
*Viral response to previous treatment was unknown in 57 patients, and 10 patients had discontinued treatment. †Data shown are median values. ‡301 missing.

Treatment

All patients received Peg-IFN α-2b (PEGINTRON; Schering-Plough, Kenilworth, NJ, USA) plus ribavirin (REBETOL; Schering-Plough) for the duration of the study of 48 weeks. Peg-IFN α-2b was given subcutaneously once weekly at a dosage of 60–150 μg/kg based on body weight (body weight 35–45 kg, 60 μg; 46–60 kg, 80 μg; 61–75 kg, 100 μg; 76–90 kg, 120 μg; 91–120 kg, 150 μg) and ribavirin was given orally twice a day at a total dose of 600–1000 mg/day based on body weight (body weight ≤60 kg, 600 mg; 60–80 kg, 800 mg; >80 kg, 1000 mg), according to a standard treatment protocol for Japanese patients.

Dose reduction

Dose modification followed, as a rule, the manufacturer's drug information according to the intensity of the haematological adverse effects. The dose of Peg-IFN α-2b was reduced to 50% of the assigned dose if the white blood cell (WBC) count declined to <1500/mm^3, the neutrophil count to <750/mm^3 or the platelet (Plt) count to <8 × $10^4/mm^3$, and was discontinued if the WBC count declined to <1000/

mm^3, the neutrophil count to $<500/mm^3$ or the Plt count to $<5 \times 10^4/mm^3$. Ribavirin was also reduced from 1000 to 600 mg, or 800 to 600 mg, or 600 to 400 mg if the haemoglobin (Hb) level decreased to <10 g/dL, and was discontinued if the Hb level decreased to <8.5 g/dL. Both Peg-IFN α-2b and ribavirin had to be discontinued if there was a need to discontinue one of the drugs. During this therapy, ferric medicine or haematopoetic growth factors, such as erythropoietin alpha, or granulocyte-macrophage colony stimulating factor (G-CSF), were not administered.

Virologic assessment and definition of virologic response

Serum HCV RNA level was quantified using the COBAS AMPLICOR HCV MONITOR test, version 2.0 (detection range 6–5000 kIU/mL; Roche Diagnotics, Branchburg, NJ, USA) and qualitatively analysed using the COBAS AMPLICOR HCV test, version 2.0 (lower limit of detection 50 IU/mL). The c-EVR was defined as the absence of detectable serum HCV RNA at treatment week 12, and SVR was defined as the absence of detectable serum HCV RNA at week 72. Patients with less than a 2-log decrease in HCV RNA level at treatment week 12 compared with the baseline had to stop treatment and were regarded as nonresponders. All patients with detectable serum HCV RNA at treatment week 24 were also considered nonresponders and excluded from further treatment.

Assessment of drug exposure

The amounts of Peg-IFN α-2b and ribavirin actually taken by each patient during the first 12 weeks of the treatment were evaluated by reviewing the medical records. The mean doses of both drugs were calculated individually as averages on the basis of body weight at baseline: Peg-IFN α-2b expressed as μg/kg/week, and ribavirin expressed as mg/kg/day.

Evaluation of impact of drug exposure on c-EVR

We evaluated the relationship between the drug exposure of both drugs and c-EVR by univariate and multivariate analysis for c-EVR, using the factors of mean administration doses of both drugs during the first 12 weeks and the factors at baseline. Furthermore, Peg-IFN α-2b dose (average dose per body weight and per week) was classified into five categories (up to 0.6 μg/kg; from 0.6 to <0.9 μg/kg; from 0.9 to <1.2 μg/kg; from 1.2 to <1.5 μg/kg; from 1.5 μg/kg and above). Ribavirin exposure was classified into four categories (up to 8 mg/kg; from 8 to <10 mg/kg; from 10 to <12 mg/kg; from 12 mg/kg and above), in order to examine the impact of Peg-IFN dose exposure on c-EVR. This impact was also evaluated based on the percentage of the total prescribed dose and compared with that based on the mean dose per body weight.

Statistical analysis

Baseline data for various demographic, biochemical and virologic characteristics of the patients are expressed as mean ± SD or median values. To analyse the relationship between baseline data including drug exposure and c-EVR, univariate analysis using the Mann–Whitney *U*-test or chi-squared test and multivariate analysis using logistic regression analysis were performed. The significance of trends in values was determined with the Mantel–Haenszel chi-square test. A two-tailed *P*-value < 0.05 was considered significant. Statistical analysis was conducted with SPSS version 15.0J (SPSS Inc., Chicago, IL, USA).

RESULTS

Progress of patients treated with Peg-IFN α-2b and ribavirin

Of the 984 patients, 81 discontinued treatment because of adverse events (n = 74) or voluntary withdrawal (n = 7) by treatment week 12. The 903 patients who completed 12 weeks of treatment were assessed for c-EVR. During 12–48 weeks of treatment, 331 of the nonresponders and nine of breakthrough discontinued treatment, as did 91 patients (adverse events, n = 71; voluntary withdrawal, n = 20). A total of 472 patients completed 48 weeks of treatment.

Drug reduction and virologic response

Peg-IFN α-2b was reduced without discontinuation in 29% (n = 266) and ribavirin was reduced without discontinuation in 40% (n = 359) of the 903 patients who completed 12 weeks of treatment. The c-EVR rate was 49% (445/903) and HCV RNA was negative at week 24 in 60% (542/903) of patients who completed 12 weeks of treatment. Of the 445 patients with c-EVR, 327 patients achieved SVR (73%). Only 7% of the 458 patients without c-EVR did so.

Impact of dose exposure of Peg-IFN α-2b and ribavirin on c-EVR

The mean dose of Peg-IFN α-2b actually taken during the first 12 weeks by each patient was 1.33 μg/kg/week (range 0.41–2.16 μg/kg/week; median 1.40 μg/kg/week) and that of ribavirin was 10.4 mg/kg/day (range 2.9–16.2 mg/kg/day; median 10.6 mg/kg/day).

The mean doses of both drugs and the factors at baseline correlated with the c-EVR were assessed by univariate and multivariate logistic regression analyses. Univariate analysis showed that factors significantly associated with c-EVR were age, sex, WBC, neutrophils, red blood cells, Hb, Plt, aspartate aminotransferase, the degree of liver fibrosis and the mean doses of Peg-IFN α-2b and ribavirin during the first 12 weeks (Table 2). The factors selected as significant by the univari-

Table 2 Univariate analysis for c-EVR among patients who completed 12 weeks treatment

Factor	c-EVR (+)	c-EVR (−)	*P*-value
n	445	458	
Age (year)	54.4 ± 10.4	57.5 ± 9.6	<0.001
Sex: male/female	267/178	237/221	0.01
Serum HCV RNA (kIU/mL)*	1500	1600	0.28
White blood cells (per mm^3)	5336 ± 1536	4818 ± 1547	<0.001
Neutrophils (per mm^3)	2789 ± 1133	2398 ± 1038	<0.001
Red blood cells ($\times 10^4/mm^3$)	450 ± 46	435 ± 49	<0.001
Haemoglobin (g/dL)	14.3 ± 1.4	13.9 ± 1.4	<0.001
Platelets ($\times 10^4/mm^3$)	17.3 ± 5.2	15.0 ± 5.6	<0.001
AST (IU/L)	62 ± 44	69 ± 44	<0.001
ALT (IU/L)	77 ± 64	80 ± 57	0.07
Histology (METAVIR)†			
Fibrosis: 0–2/3–4	273/37	247/74	<0.001
Activity: 0–1/2–3	171/139	159/162	0.16
Peg-IFN dose (μg/kg/week)‡	1.39 ± 0.22	1.28 ± 0.30	<0.001
Ribavirin dose (mg/kg/day)‡	10.6 ± 1.7	10.1 ± 2.1	0.002

c-EVR, complete early virologic response; HCV, hepatitis C virus; AST, aspartate aminotransferase; ALT, alanine aminotransferase; Peg-IFN, pegylated interferon.
*Data shown are median values. †272 missing. ‡Mean doses during 0–12 weeks.

Table 3 Multivariate analysis for c-EVR among patients who completed 12 weeks treatment

Factor	Category	Odds ratio	95% CI	*P*-value
Age	by 1 year	0.982	0.966–0.999	0.04
Sex	male/female	–	–	NS
Neutrophils	by 100/mm^3	1.017	1.002–1.033	0.03
Red blood cells	by $1 \times 10^4/mm^3$	–	–	NS
Haemoglobin	by 1 g/dL	–	–	NS
Platelets	by $1 \times 10^4/mm^3$	1.051	1.014–1.088	<0.01
AST	by 1 IU/L	–	–	NS
Fibrosis*	0–2/3–4	–	–	NS
Peg-IFN dose†	by 0.1 μg/kg/week	1.079	1.011–1.151	0.02
Ribavirin dose†	by 1 mg/kg/day	–	–	NS

95% CI, 95% confidence interval; Peg-IFN, c-EVR, complete early virologic response; pegylated interferon; N.S., No Significant difference; AST, aspartate aminotransferase.
*METAVIR fibrosis score. †Mean doses during 0–12 weeks.

ate analysis were evaluated by multivariate logistic regression analysis. The mean dose of Peg-IFN α-2b during the first 12 weeks was the independent factor for c-EVR ($P = 0.02$), apart from the neutrophils ($P = 0.03$) and Plt value at baseline ($P < 0.01$) and age ($P = 0.04$) (Table 3). In contrast, the mean dose of ribavirin during the first 12 weeks showed no correlation with c-EVR.

The c-EVR rates were 54% (137/253) and 56% (246/443) for patients who received ≥1.5 and 1.2–1.5 μg/kg/week of Peg-IFN α-2b on average during the first 12 weeks, and declined to an average rate of 38% (40/105) in patients given 0.9–1.2 μg/kg/week of Peg-IFN α-2b, and an average rate of 22% (22/102) in patients given <0.9 μg/kg/week ($P < 0.0001$) (Table 4). The c-EVR rate among the patients with ≥1.2 μg/kg/week of Peg-IFN α-2b was significantly higher than that of the patients with <1.2 μg/kg/week [≥1.2 μg/kg/week, 55% (383/696) *vs* <1.2 μg/kg/week, 30% (62/207), $P < 0.0001$].

Next, we analysed the impact of Peg-IFN α-2b on c-EVR in stratified analysis according to ribavirin dose. Figure 1 shows the relationship of c-EVR and the degree of Peg-IFN α-2b exposure for two groups of ribavirin doses: the group with ≥10.6 mg/kg/day of ribavirin and that with <10.6 mg/kg/day (10.6 mg/kg/day was the median value). In either group, the mean dose of Peg-IFN α-2b was dose-dependently correlated with c-EVR ($P < 0.0001$), and c-EVR rates were very similar in both groups if the dose categories of Peg-IFN α-2b were the same.

Table 4 The c-EVR rate according to Peg-IFN and ribavirin doses during weeks 0–12 for patients who completed 12 weeks treatment

Ribavirin dose (mg/kg/day)**	Peg-IFN α-2b dose (μg/kg/week),*				
	≥1.5	1.2–1.5	0.9–1.2	<0.9	Total
≥12	57% (60/105)	61% (22/36)	38% (6/16)	22% (2/9)	54% (90/166)
10–12	54% (46/85)	58% (154/267)	36% (14/39)	23% (11/47)	51% (225/438)
8–10	50% (25/50)	53% (52/99)	52% (15/29)	18% (4/22)	48% (96/200)
<8	46% (6/13)	44% (18/41)	24% (5/21)	21% (5/24)	34% (34/99)
Total	54% (137/253)	56% (246/443)	38% (40/105)	22% (22/102)	49% (445/903)

c-EVR, complete early virologic response; Peg-IFN, pegylated interferon.
*$P < 0.0001$ for comparison of the four Peg-IFN groups. **$P = 0.05$ for comparison of the four ribavirin groups.

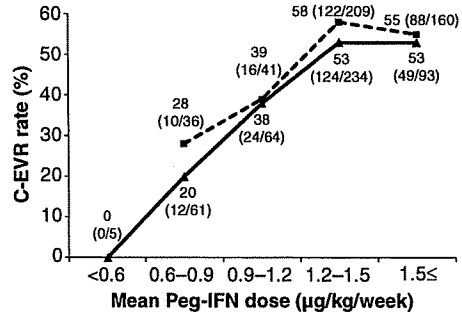

Fig. 1 Complete-EVR rate according to pegylated interferon alpha-2b (Peg-IFN α-2b) and ribavirin doses during weeks 0–12 for patients who completed 12 weeks of treatment. (-▲-) Group with the mean ribavirin dose <10.6 mg/kg/day. (··■··) Group with the mean ribavirin dose ≥10.6 mg/kg/day. The Peg-IFN α-2b dose was dose-dependently correlated with c-EVR in both groups ($P < 0.0001$). There was no significant difference between the two ribavirin-dose groups ($P = 0.19$).

c-EVR rates according to Peg-IFN α-2b drug exposure using a percentage cut off and mean dose cut off

Table 5 shows the c-EVR rates according to the category of Peg-IFN α-2b doses during the first 12 weeks based on the percentage of the total prescribed dose and the mean doses. The whole c-EVR rate was 54% (377/698) for patients who received more than 80% of the prescribed dose, and 43% (47/109) in patients given 60–80% of the prescribed dose, and 21% (21/96) in patients given <60% of the prescribed dose of Peg-IFN α-2b. Among patients given ≥80% of the prescribed dose of Peg-IFN α-2b, the c-EVR rate was significantly lower in patients given <1.2 μg/kg/week of Peg-IFN α-2b than those given ≥1.2 μg/kg/week (32% *vs* 55%, $P < 0.05$). On the other hand, even in patients given 60–80% of the prescribed dose of Peg-IFN α-2b, if they were given ≥1.2 μg/kg/week of Peg-IFN α-2b, a higher c-EVR rate was attained in comparison with those given <1.2 μg/kg/week (71% *vs* 38%, $P = 0.01$); the c-EVR rate in patients given 60–80% of the prescribed dose and ≥1.2 μg/kg/week of Peg-IFN α-2b was not inferior to that in patients given ≥80% of the prescribed dose and ≥1.2 μg/kg/week of Peg-IFN α-2b.

Impact of dose exposure of Peg-IFN α-2b during the first 12 weeks of the treatment on HCV RNA negativity at week 24 and SVR

Patients positive for HCV RNA at week 24 week during Peg-IFN α-2b and ribavirin treatment were regarded as non-responders and stopped treatment [11]. We analysed the

Table 5 The c-EVR rate according to Peg-IFN dose during weeks 0–12 based on the percentage of the planned dose and the mean doses

Peg-IFN α-2b dose (μg/kg/week)	≥80%	60–80%	<60%	Total
≥1.2	55%* (371/679)	71%** (12/17)	–	55% (383/696)
<1.2	32% (6/19)	38% (35/92)	22% (21/96)	30% (62/207)
Total	54% (377/698)	43% (47/109)	21% (21/96)	49% (445/903)

c-EVR, complete early virologic response; Peg-IFN, pegylated interferon.
*$P < 0.05$; patients with ≥1.2 μg/kg/week *vs* <1.2 μg/kg/week among the patients with more than 80% of the total prescribed dose of Peg-IFN α-2b. **$P = 0.01$; patients with ≥1.2 μg/kg/week *vs* <1.2 μg/kg/week among the patients with more than 60–80% of the total prescribed dose of Peg-IFN α-2b.

relationship between the dose exposure to Peg-IFN α-2b during the first 12 weeks and HCV RNA negative rates at week 24 or SVR in 903 patients completing 12 weeks of treatment. As a result, HCV RNA negative rates at week 24 and SVR rates declined according to the decrease in the dose of Peg-IFN α-2b during the 12 weeks of treatment; patients given ≥1.5, 1.2–1.5, 0.9–1.2 and <0.9 μg/kg/week of Peg-IFN α-2b during the first 12 weeks of the treatment showed HCV RNA negativity of 63%, 66%, 48% and 39%, respectively ($P < 0.0001$), and SVR of 46%, 43%, 30% and 20%, respectively ($P < 0.0001$).

DISCUSSION

Adherence to ribavirin was reported to be the important factor for EVR as well as that to Peg-IFN in most previous studies [2,11,12]. However, the drug exposure of Peg-IFN α-2b and ribavirin had not been analysed independently with respect to their individual influence on the anti-viral effect in these studies. Adherence to both drugs may be related factors, i.e. most patients who can tolerate a high dose of Peg-IFN are in good condition and thus can also receive a high dose of ribavirin. In the present study, the impact of the dose of Peg-IFN α-2b and ribavirin on the anti-viral effect was evaluated by multivariate logistic regression analysis, using the mean administration doses of both drugs during the first 12 weeks and baseline factors. As a result, the dose exposure of Peg-IFN α-2b was found to be the significant factor affecting c-EVR as well as baseline factors such as age, neutrophils and Plt values, but not ribavirin. This suggests that the c-EVR rate can be raised by maintaining the dose of Peg-IFN α-2b during the first 12 weeks in patients with disadvantageous factors at baseline. In fact, the c-EVR rate was higher in those who received ≥1.2 μg/kg of Peg-IFN α-2b than in those given <1.2 μg/kg of Peg-IFN α-2b for aged patients over 60 years of age (≥1.2 μg/kg; 46% *vs* <1.2 μg/kg; 28%, $P < 0.01$) or for patients with a low Plt value ($<12 \times 10^4/mm^3$)(≥1.2 μg/kg; 45% *vs* <1.2 μg/kg; 22%, $P < 0.001$). Therefore, a marked dose reduction of Peg-IFN α-2b should not be risked at the start even for aged patients or patients with lower Plt value, which is indicative of advanced fibrosis. The administration of ≥1.2 μg/kg/week of Peg-IFN α-2b is desirable as a starting dose for achieving c-EVR even in these patients: that of <1.2 μg/kg/week can lead to a non-viral response or a late viral response. Independent evaluation of the c-EVR rate according to the degree of the ribavirin dose showed a stepwise decline as the total cumulative dose of Peg-IFN α-2b decreased. Therefore, the dose of Peg-IFN α-2b should be maintained as high as possible even in patients who have to reduce Peg-IFN α-2b to <1.2 μg/kg/week. Using G-CSF for patients who develop severe neutropenia and are forced to decrease Peg-IFN can be beneficial, especially in the first 12 weeks.

The goal of 80% of the planned drug dosage for 80% of the assigned duration was derived from an adherence criterion that had been adopted previously for assessment of the efficacy of other pharmaceutical agents, such as drugs to treat cancer and human immunodeficiency virus [16]. However, in Peg-IFN plus ribavirin therapy for patients with CH-C, the planned administration dose [17,18] differs on a body weight basis by 27% for Peg-IFN α-2b and 40% for ribavirin among patients of 50–100 kg of body weight, which would be equivalent to the same rate differences for 80% of the planned drug dosage. In detail, the target dose of Peg-IFN α-2b scheduled to be administered is 1.5 μg/kg, but the usual dose for the individual patient is from 1.28 to 1.76 μg/kg/week based on body weight among patients weighing 50–100 kg according to the practice guidelines of the American Association for the Study of Liver Diseases and the manufacturer's drug information in the USA and Europe [17,18]. The range of ribavirin dose per kg of body weight is from 12 to 20 mg/kg/day. Therefore, in this study, the drug exposure was assessed from the average dose per kg of body weight.

In the evaluation of c-EVR rates according to Peg-IFN α-2b drug exposure using a percentage cut off and mean dose cut off in this study, the c-EVR rate of patients given <1.2 μg/kg/week of Peg-IFN α-2b was low (32%) even in those who received ≥80% of the total planned doses of Peg-IFN α-2b. If given ≥1.2 μg/kg/week of Peg-IFN α-2b, the c-EVR rate (71%) in patients who received 60–80% of the total doses was not inferior to that in patients given ≥80% of the total dose of Peg-IFN α-2b (54%). This means that patients whose starting dose of Peg-IFN α-2b is <1.5 μg/kg/week should not have their dosage reduced to 80% of the planned dose (<1.2 μg/kg/week) in order to have a higher probability of c-EVR, while those given ≥1.5 μg/kg/week of Peg-IFN α-2b at the start can have their dosage reduced to 80% (≥1.2 μg/kg/week) without lowering the c-EVR rate. Thus, the drug dose on a body weight basis itself should be examined as an index of the drug exposure in order to evaluate the anti-viral effect of both drugs accurately for patients with CH-C.

As for the impact of the drug exposure to ribavirin on c-EVR, the drug dose of ribavirin during the first 12 weeks was shown to have no relationship with the c-EVR rate, although it was precisely evaluated in this study, using doses actually taken on body weight. However, ribavirin can be more effective for decreasing the viral relapse after interferon or Peg-IFN α-2b and ribavirin combination therapy in patients with CH-C genotype 1 [2,3,19–24]. Recently, Shiffman *et al.* [15] have reported that a higher starting dose of ribavirin (1000–1600 mg/day) plus a regular dose of Peg-IFN α-2b with epoetin was associated with a lower relapse rate in treatment with CH-C genotype 1. Considering the viral relapse after treatment, it is thought that the ribavirin dose should not be reduced quickly in patients with mild side effects, even though it does not affect c-EVR. In fact, among the patients who attained c-EVR, a higher rate of viral relapse was found in the patients given <10 mg/kg/day of the mean ribavirin dose during 48 weeks in comparison

with those given ≥10 mg/kg/day of the mean ribavirin dose in this study [26.9% (49/182) *vs* 12.4% (26/209), $P < 0.001$] (data not shown). It seems possible to start ribavirin at a lower dose and increase it by degrees with monitoring of Hb level during treatment of patients with mild anaemia or ischemic heart disease, because the ribavirin dose appears to affect the viral relapse as the total dose over 48 weeks, not during the first 12 weeks.

In conclusion, our results have demonstrated that Peg-IFN α-2b is dose-dependently correlated with c-EVR and maintaining as high a drug dose of Peg-IFN α-2b as possible (≥1.2 μg/kg/week) during the first 12 weeks can yield higher c-EVR rates, leading to better treatment outcomes for patients with CH-C genotype 1.

ACKNOWLEDGMENTS AND DISCLOSURES

Other institutions and participants in the Osaka Liver Forum are: K Katayama, Osaka Koseinenkin Hospital; H Fukui, Yao Municipal Hospital; Y Doi, Otemae Hospital; A Kaneko, NTT West Osaka Hospital; T Kashihara, Itami City Hospital; K Kiriyama, Ashiya Municipal Hospital; T Nagase, Suita Municipal Hospital; M Inada, Toyonaka Municipal Hospital; K Fujimoto, National Hospital Organization Minami Wakayama Medical Center; K Suzuki, Saiseikai Senri Hospital; H Ogawa, Nishinomiya Municipal Central Hospital; S Kubota, Kano General Hospital; M Nishiuchi, Saso Hospital; and N Imaizumi, Osaka Kaisei Hospital.

This work was supported by a Grant-in-Aid for Research on Hepatitis and BSE from Ministry of Health Labour and Welfare of Japan, and Scientific Research from the Ministry of Education, Science, and Culture of Japan.

REFERENCES

1 Hayashi N, Takehara T. Antiviral therapy for chronic hepatitis C: past, present, and future. *J Gastroenterol* 2006; 41: 17–27.
2 Manns MP, McHutchison JG, Gordon SC *et al.* Peginterferon alfa-2b plus ribavirin compared with interferon alfa-2b plus ribavirin for initial treatment of chronic hepatitis C: a randomised trial. *Lancet* 2001; 358: 958–965.
3 Fried MW, Shiffman ML, Reddy KR *et al.* Peginterferon alfa-2a plus ribavirin for chronic hepatitis C virus infection. *N Engl J Med* 2002; 347: 975–982.
4 Hadziyannis SJ, Sette H Jr, Morgan TR *et al.* Peginterferon-alpha2a and ribavirin combination therapy in chronic hepatitis C: a randomized study of treatment duration and ribavirin dose. *Ann Intern Med* 2004; 140: 346–355.
5 Zeuzem S, Hultcrantz R, Bourliere M *et al.* Peginterferon alfa-2b plus ribavirin for treatment of chronic hepatitis C in previously untreated patients infected with HCV genotypes 2 or 3. *J Hepatol* 2004; 40: 993–999.
6 Hiramatsu N, Hayashi N, Kasahara A *et al.* Improvement of liver fibrosis in chronic hepatitis C patients treated with natural interferon alpha. *J Hepatol* 1995; 22: 135–142.
7 Kasahara A, Hayashi N, Mochizuki K *et al.* Risk factors for hepatocellular carcinoma and its incidence after interferon treatment in patients with chronic hepatitis C. Osaka Liver Disease Study Group. *Hepatology* 1998; 27: 1394–1402.
8 Ikeda K, Saitoh S, Arase Y *et al.* Effect of interferon therapy on hepatocellular carcinogenesis in patients with chronic hepatitis type C: a long-term observation study of 1,643 patients using statistical bias correction with proportional hazard analysis. *Hepatology* 1999; 29: 1124–1130.
9 Kasahara A, Tanaka H, Okanoue T *et al.* Interferon treatment improves survival in chronic hepatitis C patients showing biochemical as well as virological responses by preventing liver-related death. *J Viral Hepatitis* 2004; 11: 148–156.
10 Imai Y, Kasahara A, Tanaka H *et al.* Interferon therapy for aged patients with chronic hepatitis C: improved survival in patients exhibiting a biochemical response. *J Gastroenterol* 2004; 39: 1069–1077.
11 Davis GL, Wong JB, McHutchison JG, Manns MP, Harvey J, Albrecht J. Early virologic response to treatment with peginterferon alfa-2b plus ribavirin in patients with chronic hepatitis C. *Hepatology* 2003; 38: 645–652.
12 McHutchison JG, Manns M, Patel K *et al.* Adherence to combination therapy enhances sustained response in genotype-1-infected patients with chronic hepatitis C. *Gastroenterology* 2002; 123: 1061–1069.
13 Shiffman ML, Ghany MG, Morgan TR *et al.* Impact of reducing peginterferon alfa-2a and ribavirin dose during retreatment in patients with chronic hepatitis C. *Gastroenterology* 2007; 132: 103–112.
14 Reddy KR, Shiffman ML, Morgan TR *et al.* Impact of ribavirin dose reductions in hepatitis C virus genotype 1 patients completing peginterferon alfa-2a/ribavirin treatment. *Clin Gastroenterol Hepatol* 2007; 5: 124–129.
15 Shiffman ML, Salvatore J, Hubbard S *et al.* Treatment of chronic hepatitis C virus genotype 1 with peginterferon, ribavirin, and epoetin alpha. *Hepatology* 2007; 46: 371–379.
16 Paterson DL, Swindells S, Mohr J *et al.* Adherence to protease inhibitor therapy and outcomes in patients with HIV infection. *Ann Intern Med* 2000; 133: 21–30.
17 Strader DB, Wright T, Thomas DL, Seeff LB. Diagnosis, management, and treatment of hepatitis C. *Hepatology* 2004; 39: 1147–1171.
18 Dienstag JL, McHutchison JG. American Gastroenterological Association medical position statement on the management of hepatitis C. *Gastroenterology* 2006; 130: 225–230.
19 Poynard T, Marcellin P, Lee SS *et al.* Randomised trial of interferon alpha2b plus ribavirin for 48 weeks or for 24 weeks versus interferon alpha2b plus placebo for 48 weeks for treatment of chronic infection with hepatitis C virus. International Hepatitis Interventional Therapy Group (IHIT). *Lancet* 1998; 352: 1426–1432.
20 McHutchison JG, Gordon SC, Schiff ER *et al.* Interferon alfa-2b alone or in combination with ribavirin as initial treatment for chronic hepatitis C. Hepatitis Interventional Therapy Group. *N Engl J Med* 1998; 339: 1485–1492.
21 Davis GL, Esteban-Mur R, Rustgi V *et al.* Interferon alfa-2b alone or in combination with ribavirin for the treatment of relapse of chronic hepatitis C. International Hepatitis Interventional Therapy Group. *N Engl J Med* 1998; 339: 1493–1499.

22 Hiramatsu N, Kasahara A, Nakanishi F *et al.* The significance of interferon and ribavirin combination therapy followed by interferon monotherapy for patients with chronic hepatitis C in Japan. *Hepatol Res* 2004; 29: 142–147.
23 Bronowicki JP, Ouzan D, Asselah T *et al.* Effect of ribavirin in genotype 1 patients with hepatitis C responding to pegylated interferon alfa-2a plus ribavirin. *Gastroenterology* 2006; 131: 1040–1048.
24 Hiramatsu N, Oze T, Yakushijin T, *et al.* Ribavirin dose reduction raises relapse rate dose-dependently in genotype 1 patients with hepatitis C responding to pegylated interferon alfa-2b plus ribavirin. *J Viral Hepat* 2009; In press.

LGP2 is a positive regulator of RIG-I– and MDA5-mediated antiviral responses

Takashi Satoh[a,1], Hiroki Kato[a,1,2], Yutaro Kumagai[a], Mitsutoshi Yoneyama[b,c], Shintaro Sato[a,3], Kazufumi Matsushita[a], Tohru Tsujimura[d], Takashi Fujita[b], Shizuo Akira[a,4], and Osamu Takeuchi[a]

[a]Laboratory of Host Defense, WPI Immunology Frontier Research Center, Research Institute for Microbial Diseases, Osaka University, Osaka 565-0871, Japan; [b]Department of Genetics and Molecular Biology, Institute for Virus Research, and Laboratory of Molecular Cell Biology, Graduate School of Biostudies, Kyoto University, Kyoto 606-8507, Japan; [c]PRESTO, Japan Science and Technology Agency, Saitama, Japan; and [d]Department of Pathology, Hyogo College of Medicine, Hyogo 663-8501, Japan

Contributed by Shizuo Akira, November 10, 2009 (sent for review October 30, 2009)

RNA virus infection is recognized by retinoic acid-inducible gene (RIG)-I–like receptors (RLRs), RIG-I, and melanoma differentiation–associated gene 5 (MDA5) in the cytoplasm. RLRs are comprised of N-terminal caspase-recruitment domains (CARDs) and a DExD/H-box helicase domain. The third member of the RLR family, LGP2, lacks any CARDs and was originally identified as a negative regulator of RLR signaling. In the present study, we generated mice lacking LGP2 and found that LGP2 was required for RIG-I– and MDA5-mediated antiviral responses. In particular, LGP2 was essential for type I IFN production in response to picornaviridae infection. Overexpression of the CARDs from RIG-I and MDA5 in *Lgp2*$^{-/-}$ fibroblasts activated the IFN-β promoter, suggesting that LGP2 acts upstream of RIG-I and MDA5. We further examined the role of the LGP2 helicase domain by generating mice harboring a point mutation of Lys-30 to Ala (*Lgp2*$^{K30A/K30A}$) that abrogated the LGP2 ATPase activity. *Lgp2*$^{K30A/K30A}$ dendritic cells showed impaired IFN-β productions in response to various RNA viruses to extents similar to those of *Lgp2*$^{-/-}$ cells. *Lgp2*$^{-/-}$ and *Lgp2*$^{K30A/K30A}$ mice were highly susceptible to encephalomyocarditis virus infection. Nevertheless, LGP2 and its ATPase activity were dispensable for the responses to synthetic RNA ligands for MDA5 and RIG-I. Taken together, the present data suggest that LGP2 facilitates viral RNA recognition by RIG-I and MDA5 through its ATPase domain.

innate immunity | type I interferon | virus infection

RNA virus infection is initially recognized by host pattern recognition receptors, including retinoic acid-inducible gene (RIG)-I–like receptors (RLRs) and Toll-like receptors (TLRs), which induce antiviral responses such as the productions of type I IFNs and proinflammatory cytokines (1–4). The RLR family comprises RIG-I, melanoma differentiation-associated gene 5 (MDA5) and LGP2. RLRs harbor a central DExD/H-box helicase domain and a C-terminal regulatory domain (RD). RIG-I and MDA5 also contain two N-terminal caspase recruitment domains (CARDs), whereas LGP2 does not. RIG-I recognizes relatively short double-stranded (ds) RNAs (up to 1 kb), and the presence of a 5′ triphosphate end greatly potentiates its type I IFN-inducing activity (5–7). On the other hand, MDA5 detects long dsRNAs (more than 2 kb), such as polyinosinic polycytidylic acid (poly I:C). Analyses of *Rig-I*–deficient (*Rig-I*$^{-/-}$) and *Mda5*$^{-/-}$ mice have shown that RIG-I is essential for the production of type I IFNs in response to various RNA viruses, including vesicular stomatitis virus (VSV), Sendai virus (SeV), Japanese encephalitis virus (JEV), and influenza virus, whereas MDA5 is critical for the detection of picornaviridae such as encephalomyocarditis virus (EMCV) and mengovirus (8, 9). Some RNA viruses such as West Nile virus and reovirus are recognized by both RIG-I and MDA5 (10, 11). RIG-I is also reported to be involved in the recognition of foreign DNA in the cytoplasm through transcription of the DNA to dsRNA by polymerase III (12, 13).

The C-terminal RDs of RLRs are responsible for binding to dsRNAs (3). However, the functions of the helicase domains of the RLR family members have not yet been clarified. Although the RIG-I helicase domain has the ability to unwind dsRNA, this activity is not correlated with the level of IFN production (14). A recent report proposed that the RIG-I ATPase activity is required for translocation of RIG-I on dsRNA (15). The N-terminal CARDs of RIG-I and MDA5 trigger intracellular signaling pathways via IFN-β promoter stimulator (IPS)–1 (also known as MAVS, VISA, or CARDIF), an adaptor molecule possessing an N-terminal CARD (16). IPS-1 subsequently activates two IκB kinase (IKK)–related kinases, IKK-*i*, and TANK-binding kinase 1 (TBK1). These kinases phosphorylate IFN-regulatory factor (IRF) 3 and IRF7, which activate the transcription of genes encoding type I IFNs and IFN-inducible genes. The produced type I IFNs alert the surrounding cells by triggering signaling cascades that lead to phosphorylation and nuclear translocation of STAT1 (1, 2).

The third RLR family member LGP2, also known as Dhx58, harbors a DExD/H-box helicase domain and a C-terminal RD but lacks any CARDs (17). In vitro studies have suggested that LGP2 negatively regulates RIG-I–mediated dsRNA recognition (18). Several models have been proposed for the mechanisms of this inhibition. The first model is that LGP2 binds to viral dsRNA and prevents RIG-I– and MDA5-mediated recognition (18). The second model is that LGP2 inhibits multimerization of RIG-I and its interaction with IPS-1 via the RD of LGP2 (19). The third model is that LGP2 competes with IKK-*i* for recruitment to IPS-1, thereby suppressing RLR signaling (20). Structural analyses of the C-terminal domain of LGP2 have revealed that LGP2 can bind to the termini of dsRNAs more firmly than MDA5 (21–23). A previous report showed that *Lgp2*$^{-/-}$mice exhibit enhanced production of type I IFNs in response to poly I:C stimulation and VSV infection, whereas the response to EMCV is suppressed (24). Therefore, the role of LGP2 in the negative or positive regulation of RLR signaling has not yet been fully clarified.

In the present study, we generated *Lgp2*$^{-/-}$ mice and mice harboring a point mutation in the LGP2 helicase domain (K30A), and examined their responses to RNA viruses recognized by RIG-I and MDA5. Conventional dendritic cells (cDCs) and mouse embryonic fibroblasts (MEFs) obtained from *Lgp2*$^{-/-}$ mice showed severely impaired IFN responses to infections with picornaviruses, which are recognized by MDA5. Furthermore,

Author contributions: T.S., H.K., S.A., and O.T. designed research; T.S., H.K., Y.K., S.S., K.M., and T.T. performed research; M.Y. and T.F. contributed new reagents/analytic tools; T.S., H.K., T.T., S.A., and O.T. analyzed data; and S.A. and O.T. wrote the paper.

The authors declare no conflict of interest.

See Commentary on page 1261.

[1]T.S. and H.K. contributed equally to this work.

[2]Present address: Program in Molecular Medicine, University of Massachusetts, Worcester, MA 01605.

[3]Present address: Division of Mucosal Immunology, Department of Microbiology and Immunology, Institute of Medical Science, University of Tokyo, Tokyo 108-8639, Japan.

[4]To whom correspondence should be addressed. E-mail: sakira@biken.osaka-u.ac.jp.

This article contains supporting information online at www.pnas.org/cgi/content/full/0912986107/DCSupplemental.

www.pnas.org/cgi/doi/10.1073/pnas.0912986107

the responses to viruses recognized by RIG-I were also impaired in $Lgp2^{-/-}$ cells. In contrast, the IFN productions in response to synthetic RNAs, poly I:C and RNA synthesized by T7 polymerase, were comparable between wild-type (WT) and $Lgp2^{-/-}$ or $Lgp2^{K30A/K30A}$ cells. $Lgp2^{-/-}$ and $Lgp2^{K30A/K30A}$ mice were highly susceptible to infection with EMCV. Taken together, the present results demonstrate that LGP2 acts as a positive, but not negative, regulator of RIG-I– and MDA5-mediated viral recognition.

Results

Generation of Mice Lacking Lgp2. To investigate the physiological role of LGP2 in vivo, we established $Lgp2^{-/-}$ mice (Fig. S1 *A* and *B*). As reported previously, the expression of *Lgp2* mRNA was highly induced in response to IFN-β stimulation in MEFs (Fig. S1*C*) (17). Expression of *Lgp2* mRNA was not detected in $Lgp2^{-/-}$ MEFs, whereas the expression levels of *Rig-I* and *Mda5* mRNAs were comparable between WT and $Lgp2^{-/-}$ cells (Fig. S1*C*). The $Lgp2^{-/-}$ progenies obtained from $Lgp2^{+/-}$ intercrosses were lower than the expected Mendelian ratio (Fig. S2*A*), indicating that homozygous mutations of the *Lgp2* gene cause embryonic lethality at a high frequency. In addition, adult female $Lgp2^{-/-}$ mice showed an enlarged uterus filled with fluid resulting from vaginal atresia (Fig. S2 *B* and *C*).

Role of LGP2 in Type I IFN and Cytokine Productions in Response to RNA Viruses. First, we examined the production of IFN-β in cDCs derived from bone marrow (BM) in the presence of GM-CSF after infection with a variety of RNA viruses (Fig. 1). The productions of IFN-β in response to picornaviridae, EMCV, and mengovirus were severely impaired in $Lgp2^{-/-}$ cDCs compared with WT cells (Fig. 1*A*). IL-6 production induced by EMCV infection was also severely impaired in $Lgp2^{-/-}$ cells (Fig. 1*B*). Furthermore, LGP2 was involved in the productions of IFN-β in response to several RNA viruses recognized by RIG-I, such as VSV, SeV, and JEV (Fig. 1*A*). IFN-β production in response to reovirus, a dsRNA virus, was also impaired in $Lgp2^{-/-}$ cells (Fig. 1*A*). In contrast, the IFN-β productions in response to infection with influenza virus were comparable between WT and $Lgp2^{-/-}$ cDCs (Fig. 1*A*). Stimulation with CpG-DNA, a TLR9 ligand, induced comparable amounts of IFN-β in WT and $Lgp2^{-/-}$ cells (Fig. 1*A*).

Next, we examined whether the defect in type I IFN production in response to EMCV was controlled at the mRNA level. The expressions of the genes encoding IFN-β, CXCL10 and IL-6 after infection with EMCV were severely impaired in $Lgp2^{-/-}$ macrophages (Fig. 2*A*). However, the influenza virus-induced expressions of IFN-β and CXCL10 mRNAs were comparable between WT and $Lgp2^{-/-}$ MEFs throughout the whole time course (Fig. 2*B*). Therefore, it is unlikely that LGP2 negatively regulates RIG-I–mediated responses, even during the later period of infection. These results indicate that LGP2 is involved in positive, but not negative, regulation of virus recognition by MDA5 and RIG-I, with the exception of influenza virus.

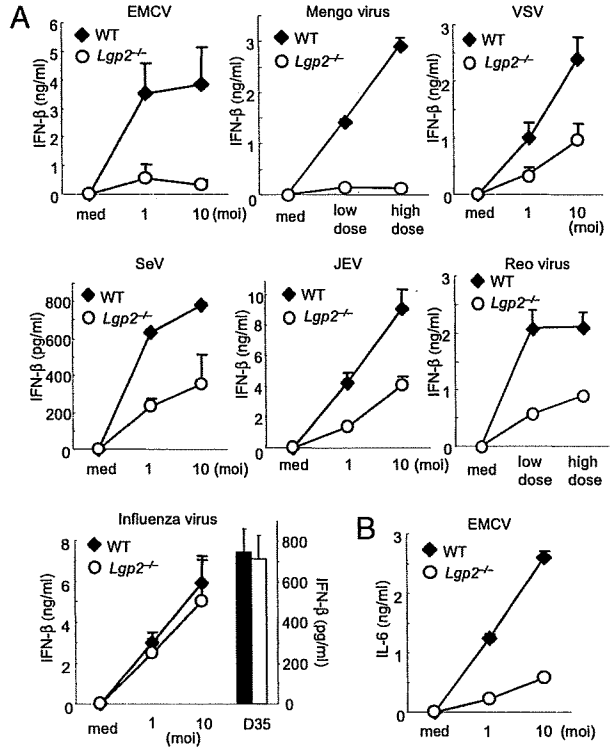

Fig. 1. Role of LGP2 in type I IFN production in response to various RNA viruses. (*A* and *B*) BM-derived cDCs from WT and $Lgp2^{-/-}$ mice were exposed to the indicated viruses or treated with 1 μM CpG-DNA (D35) for 24 h. The concentrations of IFN-β (*A*) and IL-6 (*B*) in the culture supernatants were measured by ELISA. moi, multiplicity of infection; med, medium alone. Data are shown as means ± SD and are representative of at least three independent experiments.

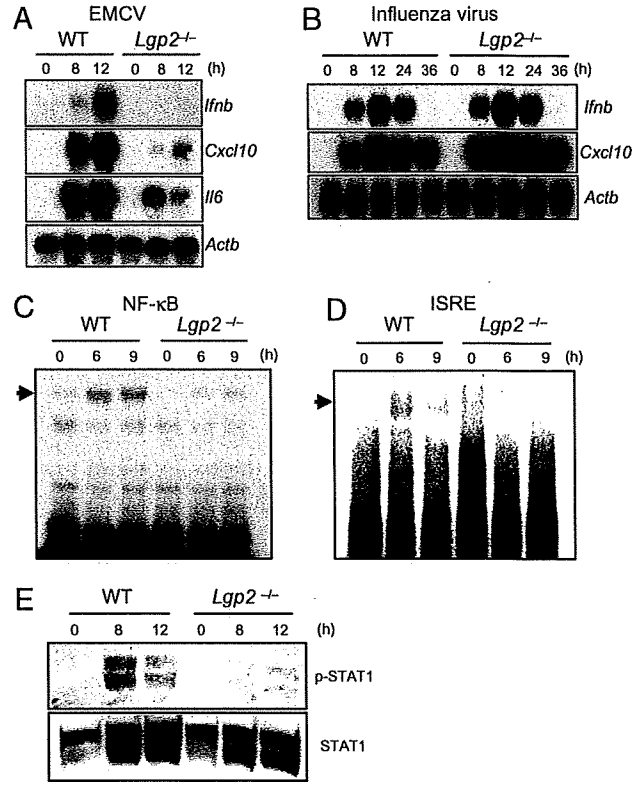

Fig. 2. Role of LGP2 in the activation of signaling pathways leading to IFN-inducible gene expression. (*A*) Total RNAs extracted from WT and $Lgp2^{-/-}$ macrophages infected with EMCV were subjected to Northern blot analyses for the expressions of *Ifnb*, *Cxcl10*, *Il6*, and *Actb* mRNAs. (*B*) WT and $Lgp2^{-/-}$ MEFs were infected with influenza virus followed by isolation of the total RNA. The expressions of *Ifnb*, *Cxcl10*, and *Actb* mRNAs were determined by Northern blot analyses. (*C* and *D*) Nuclear extracts were prepared from WT and $Lgp2^{-/-}$ macrophages infected with EMCV for the indicated periods. The binding activities of DNA to NF-κB (*C*) and ISREs (*D*) were determined by EMSAs. (*E*) Cell lysates were prepared from WT and $Lgp2^{-/-}$ macrophages infected with EMCV and probed with anti–phospho-STAT-1 and anti-STAT1 antibodies. The data are representative of at least three independent experiments.

Cell Type-Specific Involvement of LGP2 in EMCV Recognition. We previously showed that RIG-I– and MDA5-dependent RNA virus recognition occurs in cDCs but not in plasmacytoid dendritic cells (pDCs) (8). To determine whether LGP2 functions in a cell type–specific fashion, $B220^{-}CD11c^{+}$ cDCs and $CD11c^{+}B220^{+}$ pDCs were purified from WT and $Lgp2^{-/-}$ splenocytes. EMCV-induced IFN-β production was severely impaired in $Lgp2^{-/-}$ splenic cDCs compared with WT cDCs, whereas splenic pDCs from WT and $Lgp2^{-/-}$ mice produced comparable amounts of IFN-β (Fig. S3). These data indicate that LGP2 functions in cDCs but not in pDCs.

LGP2 Is Essential for Triggering RLR Signaling Pathways. To investigate whether LGP2 regulates the primary responses to RNA virus infections, we examined the activation of intracellular signaling pathways. Electrophoretic mobility shift assays (EMSAs) revealed that the activations of NF-κB and IFN-stimulated regulatory elements (ISREs) in response to EMCV infection were severely impaired in $Lgp2^{-/-}$ cells (Fig. 2 *C* and *D*). Furthermore, the phosphorylation of STAT1 was abrogated in $Lgp2^{-/-}$ cells (Fig. 2*E*). Nevertheless, the expressions of *Lgp2* in response to IFN-β treatment were not altered in $Rig\text{-}I^{-/-}$ and $Mda5^{-/-}$ cells (Fig. S4). These results suggest that LGP2 is required for the initial recognition of EMCV, leading to activation of transcription factors involved in the expression of type I IFNs.

Next, we examined whether the expression of *Lgp2* could rescue the virus-mediated IFN responses. IFN-β–dependent reporter gene expression was induced in response to EMCV infection in WT, but not in $Lgp2^{-/-}$, MEFs (Fig. 3*A*). Expression of exogenous LGP2 in $Lgp2^{-/-}$ cells restored the EMCV-induced IFN-β promoter activity as well as IFN-β production (Fig. 3 *A* and *B*). Although overexpression of either LGP2 or MDA5 alone in $Lgp2^{-/-}Mda5^{-/-}$ MEFs failed to confer EMCV-induced IFN-β promoter activity, coexpression of both LGP2 and MDA5 restored EMCV responsiveness (Fig. 3*C*). Overexpression of the CARDs from RIG-I or MDA5 in $Lgp2^{-/-}$ MEFs activated the IFN-β promoter (Fig. 3*D*), suggesting that LGP2 functions upstream of RIG-I and MDA5.

Normal IFN Responses of $LGP2^{-/-}$ cells to Exogenously Transfected RNAs. We examined the responses of $Lgp2^{-/-}$ cells to synthetic RNAs recognized by RIG-I and MDA5. Unexpectedly, WT and $Lgp2^{-/-}$ cDCs produced comparable amounts of IFN-β in response to poly I:C, in vitro–transcribed dsRNA and RNA with a 5′ triphosphate end (Tri-P) (Fig. 4*A*). Similarly, Lgp2-deficiency did not affect the IFN-β productions in response to the synthesized RNAs in fibroblasts (Fig. 4*A*). In addition, no differences were observed in the responses to the various concentrations of poly I:C examined (Fig. 4*B*). These data suggest that LGP2 is dispensable for the recognition of synthesized dsRNA and 5′ triphosphate RNA.

Function of LGP2 ATPase Domain in Type I IFN Responses to Virus Infections. The recognition of dsRNA and RNA viruses by RIG-I or MDA5 requires ATPase activity (17, 25). To examine the role of the LGP2 ATPase activity in LGP2-mediated virus recognition, we reconstituted $Lgp2^{-/-}$ MEFs with WT LGP2 or LGP2-K30A harboring a Lys-to-Ala point mutation in the Walker ATP-binding motif using a retrovirus system. Expression of WT LGP2 in $Lgp2^{-/-}$ MEFs conferred IFN-β promoter activity as well as IFN-β production in response to EMCV, whereas expression of LGP2-K30A failed to confer these responses to EMCV infection (Fig. 5 *A* and *B*).

To further examine the role of the LGP2 ATPase activity in vivo, we generated mice harboring the LGP2 K30A point mutation (Fig. S5 *A* and *B*). Expression of *Lgp2* mRNA was comparably induced in response to IFN-β stimulation in WT and $Lgp2^{K30A/K30A}$ MEFs (Fig. S5*C*). We confirmed the insertion of

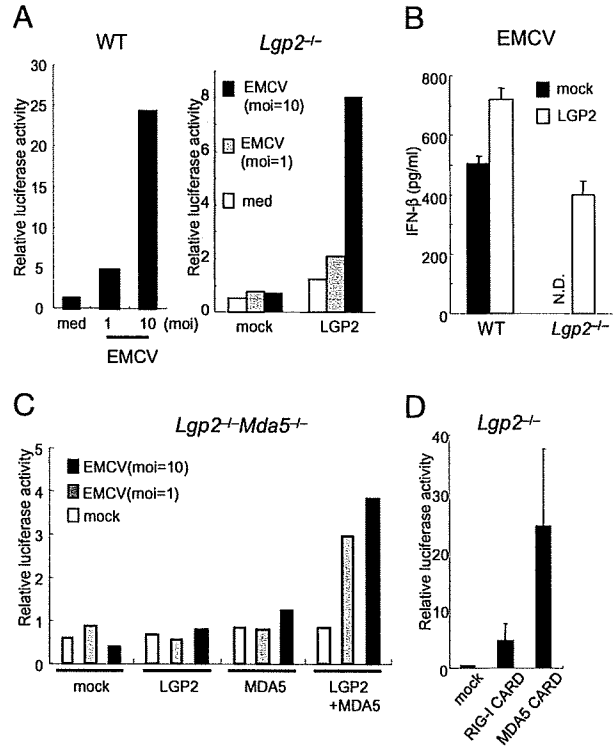

Fig. 3. LGP2 acts in the upstream of RIG-I and MDA5. (*A*) WT and $Lgp2^{-/-}$ MEFs were transiently transfected with the IFN-β promoter construct together with expression plasmids encoding LGP2. The cells were infected with EMCV for 8 h and then lysed. The cell lysates were analyzed by a luciferase assay. (*B*) WT and $Lgp2^{-/-}$ MEFs were infected with a retrovirus expressing *Lgp2*. At 2 days after infection, the cells were exposed to EMCV for 24 h. The IFN-β concentrations in the culture supernatants were measured by ELISA. N.D., not detected. (*C*) $Lgp2^{-/-}Mda5^{-/-}$ MEFs were transiently transfected with the IFN-β promoter reporter construct together with the indicated expression plasmids. After 24 h, the cells were infected with EMCV for 8 h and then lysed. The cell lysates were analyzed by a luciferase assay. (*D*) $Lgp2^{-/-}$ MEFs were transiently transfected with the IFN-β promoter construct together with expression plasmids encoding the CARDs of RIG-I or MDA5 and then lysed at 48 h after transfection. The cell lysates were analyzed by a luciferase assay.

the point mutation by sequencing analysis (Fig. S5*D*). The $Lgp2^{K30A/K30A}$ mice were born at the expected Mendelian ratio, and did not show any developmental defects. We examined the IFN-β productions in cDCs in response to infections with RNA viruses. The IFN-β productions in response to infections with EMCV, mengovirus, VSV, SeV, and reovirus, but not with influenza virus, were severely impaired in $Lgp2^{K30A/K30A}$ cDCs compared with WT cells (Fig. 5*C*). The IL-6 production in response to EMCV infection was also impaired in $Lgp2^{K30A/K30A}$ cDCs (Fig. 5*D*). The defects observed in $Lgp2^{K30A/K30A}$ cDCs were as severe as those observed in $Lgp2^{-/-}$ cDCs, suggesting that the ATPase activity of LGP2 is essential for the recognition of viruses. The productions of IFN-β in response to transfections of synthetic RNAs and poly I:C were comparable between WT and $Lgp2^{K30A/K30A}$ cells (Fig. 5*E*), further confirming that LGP2 is not involved in the responses to the transfection of synthetic RNAs. Taken together, these results indicate that the ATPase activity of LGP2 is essential for LGP2 to function as a positive regulator in MEFs. This finding is in marked contrast to in vitro experiments in which overexpression of WT LGP2 and LGP2-K30A in HEK293 cells suppressed RIG-I–mediated IFN-β promoter activity (Fig. S6), suggesting that overexpression of

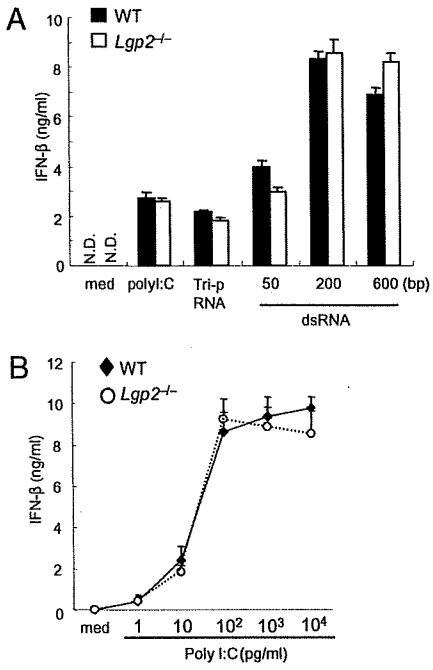

Fig. 4. Role of LGP2 in the recognition of exogenously transfected RNAs. (*A*) WT and *Lgp2*$^{-/-}$ MEFs were stimulated with triphosphate RNA, in vitro–transcribed dsRNA (1 μg/mL) or poly I:C complexed with Lipofectamine 2000 for 24 h. The IFN-β concentrations in the culture supernatants were measured by ELISA. med, medium; N.D., not detected. Data are shown as the means ± SD of triplicate samples. Similar results were obtained in three independent experiments. (*B*) WT and *Lgp2*$^{-/-}$ MEFs were transfected with the indicated amounts of poly I:C complexed with Lipofectamine 2000. The IFN-β concentrations in the culture supernatants were measured by ELISA.

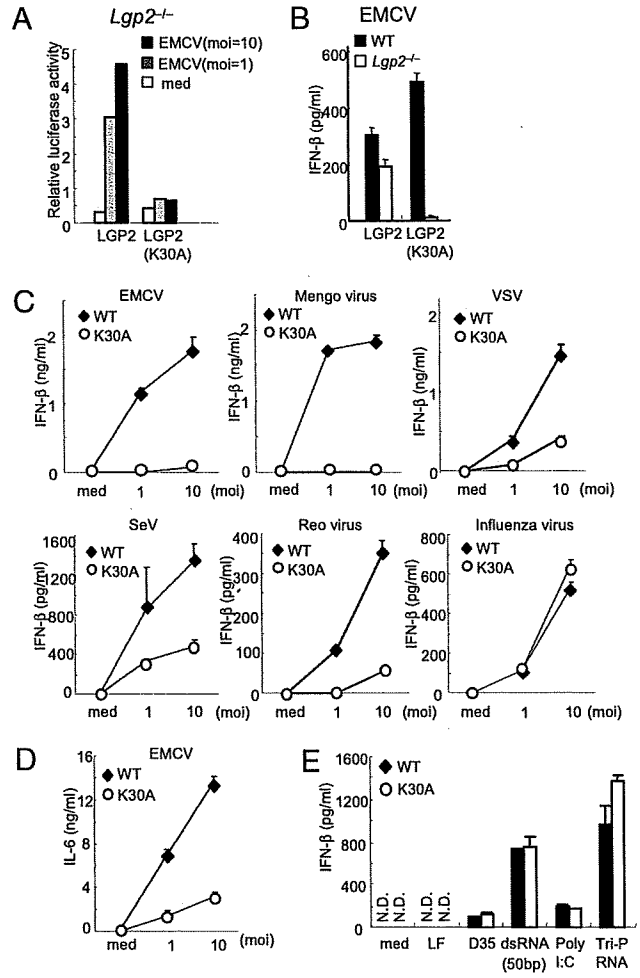

Fig. 5. Essential role of the LGP2 ATPase activity in the recognition of RNA viruses. (*A*) *Lgp2*$^{-/-}$ MEFs were transiently transfected with the IFN-β promoter construct together with expression plasmids encoding *LGP2 or LGP2* (K30A). The cells were infected with EMCV for 8 h and then lysed. The cell lysates were analyzed by a luciferase assay. (*B*) WT and *Lgp2*$^{-/-}$ MEFs were infected with retroviruses expressing *LGP2 or LGP2 (K30A)*. At 2 days after infection, the cells were exposed to EMCV for 24 h and the IFN-β concentrations in the culture supernatants were measured by ELISA. (*C* and *D*) WT and *Lgp2*$^{K30A/K30A}$ (K30A) mice were exposed to the indicated RNA viruses for 24 h. The concentrations of IFN-β (*C*) and IL-6 (*D*) in the culture supernatants were measured by ELISA. (*E*) WT and *Lgp2*$^{K30A/K30A}$ cDCs were transfected with the indicated RNAs for 24 h. The concentrations of IFN-β in the culture supernatants were measured by ELISA. moi, multiplicity of infection; med, medium alone; LF, lipofectamine alone. Data are shown as means ± SD and are representative of at least three independent experiments.

LGP2 in HEK293 cells nonspecifically inhibits the RIG-I–mediated pathway.

Role of LGP2 and Its ATPase Activity in Antiviral Host Defenses In Vivo. Finally, we assessed the role of LGP2 and its ATPase activity in antiviral responses in vivo. When *Lgp2*$^{-/-}$ mice were challenged with EMCV, IFN-β production was not detected in their sera (Fig. 6*A*). Furthermore, *Lgp2*$^{-/-}$ mice were highly susceptible to EMCV infection compared with their littermate controls (Fig. 6*C*). Consistent with the increased susceptibility to EMCV, the viral titer in the heart was remarkably higher in *Lgp2*$^{-/-}$ mice than in control mice (Fig. 6*E*). Similar to the results for *Lgp2*$^{-/-}$ mice, *Lgp2*$^{K30A/K30A}$ mice showed severe defects in IFN-β production in response to EMCV infection (Fig. 6*B*). *Lgp2*$^{K30A/K30A}$ mice were highly susceptible to infection with EMCV, with highly increased viral titers in their hearts (Fig. 6 *D* and *F*). These data indicate that LGP2 also plays a key role in the host defenses against RNA viruses recognized by MDA5 in vivo.

Discussion

The present data clearly demonstrate that LGP2 acts as a positive regulator of MDA5- and RIG-I–mediated viral recognition, except for influenza virus. These findings are in contrast to the conclusions deduced from previous in vitro studies and a report on Lgp2 knockout mice generated by another group (17, 18, 20, 24). LGP2 is particularly important for the recognition of picornaviruses, including EMCV and mengovirus, among RNA viruses. Analyses of the activation status of signaling molecules revealed that LGP2 was involved in the primary recognition of EMCV upstream of MDA5. LGP2 was also involved in the recognition of RNA viruses recognized by RIG-I, such as VSV and SeV, although the defects in the responses to these viruses observed in *Lgp2*$^{-/-}$ cells were not as severe as the defects in the responses to picornaviruses. Surprisingly, *Lgp2*$^{-/-}$ cells responded efficiently to synthetic RNA compounds, including poly I:C, dsRNA transcribed in vitro using T7 polymerase and 5′ triphosphate RNA.

Cells from *Lgp2*$^{K30A/K30A}$ mice showed severe defects in the IFN responses to RNA viruses to extents similar to those of *Lgp2*$^{-/-}$ cells. Furthermore, expression of the LGP2-K30A mutant protein in *Lgp2*$^{-/-}$ cells failed to restore the EMCV responsiveness. These results clearly demonstrate that the ATPase domain of LGP2 is a prerequisite for its function in recognizing RNA virus infection. Recent advances in studies on DExD/H-box

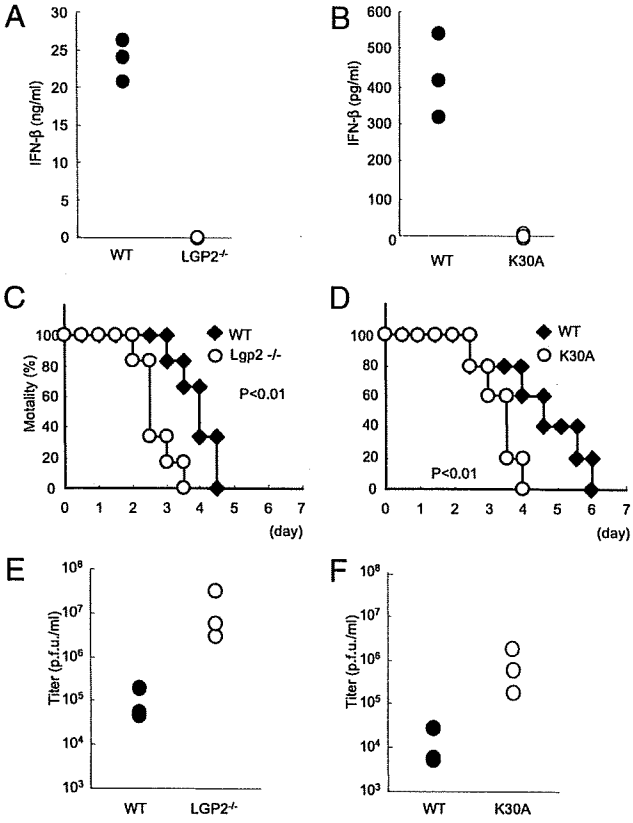

Fig. 6. Role of LGP2 in host defense against EMCV infection in vivo. (*A* and *B*) WT and littermate $Lgp2^{-/-}$ mice (*A*) or WT and littermate $Lgp2^{K30A/K30A}$ (K30A) mice (*B*) were i.v. inoculated with 1×10^7 pfu EMCV. Serum samples were obtained at 4 h after injection, and the IFN-β concentrations were determined by ELISA. (*C* and *D*) Survival rates of WT and $Lgp2^{-/-}$ mice (*C*) or WT and littermate $Lgp2^{K30A/K30A}$ mice (*D*) intraperitoneally infected with 1×10^2 pfu EMCV were monitored every 12 h for 5 days. (*E* and *F*) WT and littermate $Lgp2^{-/-}$mice (*E*) or WT and littermate $Lgp2^{K30A/K30A}$ mice (*F*) were infected i.p. with 1×10^2 pfu EMCV. After 48 h, the mice were killed and the virus titers in their hearts were determined by a plaque assay.

proteins have revealed that these proteins are involved in all aspects of RNA metabolism including translation initiation, mRNA splicing, and nuclear transport (26). Although DExD/H-box proteins, including RIG-I, are known to exhibit ATP-dependent RNA helicase activity in vitro, many DExD/H-box proteins have a more general RNA conformational change activity, rather than just a duplex-unwinding activity. In this regard, it is tempting to speculate that LGP2 functions to modify viral RNA by removing proteins from viral ribonucleoprotein (RNP) complexes or unwinding complex RNA structures to facilitate MDA5- and RIG-I–mediated recognition of dsRNA. Picornaviruses replicate in association with the cytoplasmic membranes of infected cells (27). It is therefore possible that LGP2 makes viral RNP complexes more accessible to MDA5 and RIG-I by changing their intracellular localization.

RLRs contain a C-terminal regulatory domain that is responsible for the binding to dsRNAs. The recent solution of the RLR C-terminal regulatory domain structures showed that the LGP2 and RIG-I C-terminal domains have a large basic surface, formed by the RNA-binding loop, and that the LGP2 C-terminal domain binds to the termini of dsRNAs (14, 21–23, 28). Although the MDA5 C-terminal domain also has a large basic surface, it is extensively flat because of the open conformation of the RNA-binding loop (21). Consequently, the RNA-binding activity of MDA5 is much weaker than those of RIG-I and LGP2. The present study has demonstrated that LGP2 is more profoundly required for the recognition of RNA viruses detected by MDA5 than for those detected by RIG-I. MDA5 may require LGP2 for efficient recruitment of viral dsRNAs to facilitate the initiation of signaling, and LGP2 appears to be more important for MDA5 than for RIG-I, possibly because of differences in their affinities for dsRNAs.

Although LGP2 is involved in the responses to various RNA viruses, influenza virus infection induced normal type I IFN production in $Lgp2^{-/-}$ cells. Type I IFN production in response to influenza virus was dependent on RIG-I but not on MDA5. We (5) and Pichlmair et al. (29) previously showed that phosphatase treatment of genomic RNA derived from influenza virus completely abolishes its type I IFN–inducing activity via RIG-I, indicating that a phosphate group at the 5′ end of the influenza virus genome is responsible for RIG-I–mediated recognition. Therefore, the 5′ triphosphate RNA present on viral genomes may be readily accessible to RIG-I without modification by LGP2.

Venkataraman et al. (24) reported that LGP2 acts as a negative regulator for the recognition of VSV and poly I:C, and a positive regulator for EMCV-induced IFN responses in macrophages by generating $Lgp2^{-/-}$ mice. Their results are contradictory to our present findings in terms of the responses to poly I:C and viruses recognized by RIG-I. Although we do not have a clear explanation for these discrepancies, expression of LGP2 in $Lgp2^{-/-}$ cells restored the responses to VSV and EMCV. Furthermore, we found that both $Lgp2^{-/-}$ and $Lgp2^{K30A/K30A}$ cells showed defects in IFN production in response to certain viruses recognized by RIG-I and showed normal responses to dsRNA specimens. Therefore, we believe that LGP2 acts as a positive, but not negative, regulator of RIG-I– and MDA5-dependent recognition of RNA virus infection and plays a pivotal role in antiviral responses in vivo.

Although some of the female $Lgp2^{-/-}$ mice showed a defect in the development of the vagina, $Lgp2^{K30A/K30A}$ mice did not exhibit any developmental abnormalities. Although the ATPase domain was essential for antiviral responses, the vaginal atresia was regulated by LGP2 independently of its ATPase activity. Given that $Rig\text{-}I^{-/-}$ mice showed fetal liver apoptosis at day 13, it will be interesting to analyze the role of the RIG-I ATPase activity in the control of development. Further studies are required to determine the roles of the RLR family members in controlling mammalian development.

Given that many RLR signaling molecules are inhibited by viral components, LGP2 may also be a target of the escape mechanisms exerted by various RNA viruses. Future studies aimed at identifying the mechanisms by which LGP2 modifies viral RNP complexes will help us to understand the roles of the innate immune system in intracellular virus recognition, and will lead to the development of new strategies to manipulate antiviral responses.

Materials and Methods

Generation of $Lgp2^{-/-}$ and $Lgp2^{K30A/K30A}$ Mice. The *Lgp2* gene was isolated from genomic DNA extracted from embryonic stem (ES) cells (GSI-I) by PCR. The targeting vector was constructed by replacing a 4-kb fragment encoding the *Lgp2* ORF (including the DExH/H box) with a neomycin-resistance gene cassette (*neo*), and inserting herpes simplex virus thymidine kinase (HSV-TK) driven by the PGK promoter into the genomic fragment for negative selection. After the targeting vector was transfected into ES cells, G418 and gancyclovir double-resistant colonies were selected and screened by PCR, and recombination was confirmed by Southern blotting. Homologous recombinants were microinjected into C57BL/6 female mice, and heterozygous F1 progenies were intercrossed to obtain $Lgp2^{-/-}$ mice. $Lgp2^{-/-}$ and littermate control mice were used for subsequent experiments.

A point mutation was inserted into a genomic fragment harboring the exon encoding Lys-30 of murine *Lgp2* by site-directed mutagenesis (Clontech) to replace this residue with Ala. A targeting vector was constructed with this genomic fragment and electroporated into ES cells. Homologous recombinants were selected and microinjected into C57BL/6 female mice,

and heterozygous F1 progenies were crossed with CAG-Cre transgenic mice to excise the *neo* cassette. Next, the CAG-Cre transgene was removed from $Lgp2^{+/K30A}$ mice by crossing the mice with C57BL/6 mice. $Lgp2^{K30A/K30A}$ and littermate control mice were used for subsequent experiments.

All animal experiments were carried out with the approval of the Animal Research Committee of the Research Institute for Microbial Diseases (Osaka University).

Mice, Cells, and Reagents. $Rig\text{-}I^{-/-}$ and $Lgp2^{-/-}Mda5^{-/-}$ MEFs were prepared from embryos on 129Sv and C57BL/6 backgrounds derived at 11.5 days post coitum. BM-derived DCs were generated in RPMI medium 1640 containing 10% FCS, 50 mM 2-mercaptoethanol, and 10 ng/mL GM-CSF (PeproTech). pDCs and cDCs were isolated from the spleen by MACS using anti-B220 and anti-CD11c microbeads (Miltenyi Biotech). Poly I:C was purchased from Amersham Biosciences. RNAs were complexed with the cationic lipid Lipofectamine 2000 (Invitrogen) and added to cells. A/D-type CpG-oligodeoxynucleotides (D35) were synthesized by Hokkaido System Science. In vitro–transcribed dsRNA and triphosphate RNA were described previously (5, 9). Antibodies against phospho-STAT1 and STAT1 (Cell Signaling) were used for Western blotting as described previously (8).

Viruses. VSV, VSV lacking an M protein variant (NCP), influenza virus ΔNS1, JEV, EMCV, and mengovirus were described previously (9). SeV lacking V protein (V–) was kindly provided by Dr. A. Kato. Reovirus was kindly provided by Dr. T. Dermody.

Northern Blotting. Total RNA was extracted from peritoneal macrophages infected with EMCV or MEFs infected with influenza virus using TRIzol reagent (Invitrogen). The obtained RNA was electrophoresed, transferred to nylon membranes, and hybridized with various cDNA probes. To detect the expression of *Lgp2* mRNA, a 326-bp fragment (772–1098) was used as a probe.

EMSA. Peritoneal macrophages (3×10^6) were infected with EMCV for various periods. Nuclear extracts were purified from the cells using lysis buffer (10 mM Hepes-KOH pH 7.8, 10 mM KCl, and 10 mM EDTA, pH 8.0), incubated with specific probes for NF-κB or ISRE DNA-binding sites, electrophoresed, and visualized by autoradiography.

Luciferase Assay. MEFs were transiently transfected with a reporter construct containing the IFN-β promoter together with an empty vector (Mock) or expression constructs for several genes using Lipofectamine 2000. As an internal control, the cells were transfected with a *Renilla* luciferase construct. The transfected cells were left untreated (medium alone) or infected with EMCV for 8 h. The cells were then lysed and subjected to a luciferase assay using a dual-luciferase reporter assay system (Promega) according to the manufacturer's instructions.

Retroviral Expression. Murine LGP2 and LGP2K30A cDNAs were individually cloned into the pLZR-IRES/GFP retroviral vector (30). Retroviruses were produced by transient transfection of the constructs into PlatE cells. MEFs were separately infected with the retroviruses expressing LGP2 and LGP2 (K30A). At 2 days after infection, the cells were exposed to EMCV for 24 h, and the IFN-β concentrations in the culture supernatants were measured by ELISA.

Plaque Assay. At 48 h after EMCV infection, hearts were prepared and homogenized in PBS. The virus titers in the hearts were determined by a standard plaque assay as described previously (9). After centrifugation, the supernatants were serially diluted and added to plates containing HeLa cells. Cells were overlaid with DMEM containing 1% low-melting point agarose and incubated for 48 h. The numbers of plaques were counted.

Measurement of Cytokine Production. Culture supernatants were collected, and the cytokine concentrations were measured using ELISA kits for IFN-β (PBL Biomedical Laboratories) and IL-6 (R&D Systems) according to the manufacturers' instructions.

Statistical Analysis. The statistical significance of differences between groups was determined by Student's *t* test, and survival curves were analyzed by the log-rank test. Values of $P < 0.05$ were considered to indicate statistical significance.

ACKNOWLEDGMENTS. We thank all of the colleagues in our laboratory, E. Kamada for secretarial assistance, and Y. Fujiwara, M. Kumagai, and R. Abe for technical assistance. We thank Drs. A. Kato and T. Dermody for providing viruses. This work was supported by the Special Coordination Funds of the Japanese Ministry of Education, Culture, Sports, Science and Technology, and grants from the Ministry of Health, Labour and Welfare in Japan, the Global Center of Excellence Program of Japan, and the National Institutes of Health (P01 AI070167).

1. Akira S, Uematsu S, Takeuchi O (2006) Pathogen recognition and innate immunity. *Cell* 124:783–801.
2. Honda K, Takaoka A, Taniguchi T (2006) Type I interferon [corrected] gene induction by the interferon regulatory factor family of transcription factors. *Immunity* 25:349–360.
3. Yoneyama M, Fujita T (2008) Structural mechanism of RNA recognition by the RIG-I-like receptors. *Immunity* 29:178–181.
4. Takeuchi O, Akira S (2009) Innate immunity to virus infection. *Immunol Rev* 227:75–86.
5. Kato H, et al. (2008) Length-dependent recognition of double-stranded ribonucleic acids by retinoic acid-inducible gene-I and melanoma differentiation-associated gene 5. *J Exp Med* 205:1601–1610.
6. Schlee M, et al. (2009) Recognition of 5′ triphosphate by RIG-I helicase requires short blunt double-stranded RNA as contained in panhandle of negative-strand virus. *Immunity* 31: 25–34.
7. Schmidt A, et al. (2009) 5′-triphosphate RNA requires base-paired structures to activate antiviral signaling via RIG-I. *Proc Natl Acad Sci USA* 106:12067–12072.
8. Kato H, et al. (2005) Cell type-specific involvement of RIG-I in antiviral response. *Immunity* 23:19–28.
9. Kato H, et al. (2006) Differential roles of MDA5 and RIG-I helicases in the recognition of RNA viruses. *Nature* 441:101–105.
10. Fredericksen BL, Keller BC, Fornek J, Katze MG, Gale M Jr (2008) Establishment and maintenance of the innate antiviral response to West Nile Virus involves both RIG-I and MDA5 signaling through IPS-1. *J Virol* 82:609–616.
11. Loo YM, et al. (2008) Distinct RIG-I and MDA5 signaling by RNA viruses in innate immunity. *J Virol* 82:335–345.
12. Chiu YH, Macmillan JB, Chen ZJ (2009) RNA polymerase III detects cytosolic DNA and induces type I interferons through the RIG-I pathway. *Cell* 138:576–591.
13. Ablasser A, et al. (2009) RIG-I-dependent sensing of poly(dA:dT) through the induction of an RNA polymerase III-transcribed RNA intermediate. *Nat Immunol* 10: 1065–1072.
14. Takahasi K, et al. (2008) Nonself RNA-sensing mechanism of RIG-I helicase and activation of antiviral immune responses. *Mol Cell* 29:428–440.
15. Myong S, et al. (2009) Cytosolic viral sensor RIG-I is a 5′-triphosphate-dependent translocase on double-stranded RNA. *Science* 323:1070–1074.
16. Kawai T, et al. (2005) IPS-1, an adaptor triggering RIG-I- and Mda5-mediated type I interferon induction. *Nat Immunol* 6:981–988.
17. Yoneyama M, et al. (2005) Shared and unique functions of the DExD/H-box helicases RIG-I, MDA5, and LGP2 in antiviral innate immunity. *J Immunol* 175:2851–2858.
18. Rothenfusser S, et al. (2005) The RNA helicase Lgp2 inhibits TLR-independent sensing of viral replication by retinoic acid-inducible gene-I. *J Immunol* 175:5260–5268.
19. Saito T, et al. (2007) Regulation of innate antiviral defenses through a shared repressor domain in RIG-I and LGP2. *Proc Natl Acad Sci USA* 104:582–587.
20. Komuro A, Horvath CM (2006) RNA- and virus-independent inhibition of antiviral signaling by RNA helicase LGP2. *J Virol* 80:12332–12342.
21. Takahasi K, et al. (2009) Solution structures of cytosolic RNA sensor MDA5 and LGP2 C-terminal domains: Identification of the RNA recognition loop in RIG-I-like receptors. *J Biol Chem* 284:17465–17474.
22. Li X, et al. (2009) The RIG-I-like receptor LGP2 recognizes the termini of double-stranded RNA. *J Biol Chem* 284:13881–13891.
23. Pippig DA, et al. (2009) The regulatory domain of the RIG-I family ATPase LGP2 senses double-stranded RNA. *Nucleic Acids Res* 37:2014–2025.
24. Venkataraman T, et al. (2007) Loss of DExD/H box RNA helicase LGP2 manifests disparate antiviral responses. *J Immunol* 178:6444–6455.
25. Yoneyama M, et al. (2004) The RNA helicase RIG-I has an essential function in double-stranded RNA-induced innate antiviral responses. *Nat Immunol* 5:730–737.
26. Linder P (2006) Dead-box proteins: A family affair—active and passive players in RNP-remodeling. *Nucleic Acids Res* 34:4168–4180.
27. Salonen A, Ahola T, Kääriäinen L (2005) Viral RNA replication in association with cellular membranes. *Curr Top Microbiol Immunol* 285:139–173.
28. Cui S, et al. (2008) The C-terminal regulatory domain is the RNA 5′-triphosphate sensor of RIG-I. *Mol Cell* 29:169–179.
29. Pichlmair A, et al. (2006) RIG-I-mediated antiviral responses to single-stranded RNA bearing 5′-phosphates. *Science* 314:997–1001.
30. Ruiz-Vela A, et al. (2001) Transplanted long-term cultured pre-BI cells expressing calpastatin are resistant to B cell receptor-induced apoptosis. *J Exp Med* 194:247–254.

Vol 458|30 April 2009|doi:10.1038/nature07924

LETTERS

Zc3h12a is an RNase essential for controlling immune responses by regulating mRNA decay

Kazufumi Matsushita[1,3]*, Osamu Takeuchi[1,3]*, Daron M. Standley[2], Yutaro Kumagai[1,3], Tatsukata Kawagoe[1,3], Tohru Miyake[1,3], Takashi Satoh[1,3], Hiroki Kato[1,3], Tohru Tsujimura[4], Haruki Nakamura[5] & Shizuo Akira[1,3]

Toll-like receptors (TLRs) recognize microbial components, and evoke inflammation and immune responses[1–3]. TLR stimulation activates complex gene expression networks that regulate the magnitude and duration of the immune reaction. Here we identify the TLR-inducible gene *Zc3h12a* as an immune response modifier that has an essential role in preventing immune disorders. *Zc3h12a*-deficient mice suffered from severe anaemia, and most died within 12 weeks. *Zc3h12a*$^{-/-}$ mice also showed augmented serum immunoglobulin levels and autoantibody production, together with a greatly increased number of plasma cells, as well as infiltration of plasma cells to the lung. Most *Zc3h12a*$^{-/-}$ splenic T cells showed effector/memory characteristics and produced interferon-γ in response to T-cell receptor stimulation. Macrophages from *Zc3h12a*$^{-/-}$ mice showed highly increased production of interleukin (IL)-6 and IL-12p40 (also known as IL12b), but not TNF, in response to TLR ligands. Although the activation of TLR signalling pathways was normal, *Il6* messenger RNA decay was severely impaired in *Zc3h12a*$^{-/-}$ macrophages. Overexpression of Zc3h12a accelerated *Il6* mRNA degradation via its 3′-untranslated region (UTR), and destabilized RNAs with 3′-UTRs for genes including *Il6*, *Il12p40* and the calcitonin receptor gene *Calcr*. Zc3h12a contains a putative amino-terminal nuclease domain, and the expressed protein had RNase activity, consistent with a role in the decay of *Il6* mRNA. Together, these results indicate that Zc3h12a is an essential RNase that prevents immune disorders by directly controlling the stability of a set of inflammatory genes.

The innate immune responses induced by TLRs are tightly controlled, because aberrant activation of TLR responses is harmful to the host, resulting in inflammatory diseases[1–3]. TLR signalling induces the expression of several genes, although only some of these genes have been functionally characterized as immune response modifiers. Therefore, investigation of TLR-inducible genes is important for clarifying the control mechanisms of innate immune reactions. To examine TLR-induced gene expression comprehensively, we performed microarray analysis using mouse macrophages from wild-type, *Myd88*$^{-/-}$ and *Trif*$^{-/-}$ (also known as *Ticam1*$^{-/-}$) mice stimulated with lipopolysaccharide (LPS), a TLR4 ligand. We selected 214 genes in which the expression was induced more than twofold either at 1 or 4 h after stimulation in wild-type cells. Hierarchical clustering of these LPS-inducible genes showed that they could be classified into three major clusters (Supplementary Fig. 1a). Among the clusters, genes in cluster III were rapidly induced in a MyD88-dependent manner. This cluster contained, among others, *Tnf*, *Nfkbiz* and *Zfp36*. Cluster III also contained the gene encoding Zc3h12a (Supplementary Fig. 1b). Northern blot analysis confirmed that *Zc3h12a* mRNA was rapidly induced in mouse macrophages after LPS stimulation and gradually decreased with time (Supplementary Fig. 1c). Zc3h12a has a CCCH-type zinc-finger motif, and forms a family with the homologous proteins Zc3h12b, Zc3h12c and Zc3h12d. Fractionation experiments showed that the Zc3h12a protein is mainly localized in the cytoplasm, rather than in the nucleus (Supplementary Fig. 1d).

To investigate the functional roles of Zc3h12a in the control of immune responses *in vivo*, we generated *Zc3h12a*-deficient mice (Supplementary Fig. 2a and 2b). PCR with reverse transcription (RT–PCR) analysis confirmed that the expression of *Zc3h12a* was abrogated in *Zc3h12a*$^{-/-}$ macrophages (Supplementary Fig. 2c). Although *Zc3h12a*$^{-/-}$ mice are born in a Mendelian ratio, they showed growth retardation, and most of the mice spontaneously died within 12 weeks of birth (Fig. 1a). *Zc3h12a*$^{-/-}$ mice showed severe splenomegaly and lymphoadenopathy (Fig. 1b). Histological examination revealed infiltration of plasma cells in the lung, paraepithelium of the bile duct and pancreas (Fig. 1c and Supplementary Fig. 3). Plasma cells also accumulated in *Zc3h12a*$^{-/-}$ lymph nodes and spleens (Fig. 1c). In the lymph nodes, granuloma formation was observed leading to the generation of giant cells with fused macrophages. Nevertheless, inflammatory changes were not observed in either the intestine or the joints of *Zc3h12a*$^{-/-}$ mice (data not shown).

Zc3h12a$^{-/-}$ mice suffered from severe anaemia, together with an increase in white blood cells and platelets (Fig. 1d). Furthermore, *Zc3h12a*$^{-/-}$ mice developed hyperimmunoglobulinemia of all immunoglobulin isotypes tested (Fig. 1e), and plasma cells infiltrated in the lung interstitial tissues were readily stained with anti-IgG or anti-IgA antibodies (Fig. 1g). Production of anti-nuclear antibodies and anti-double-stranded-DNA antibodies were detected in *Zc3h12a*$^{-/-}$ mice (Fig. 1f). Flow cytometric analysis showed that about 70% of CD19^{+} B cells were IgM^{-} IgD^{-}, but immunoglobulin^{+}, indicating that most *Zc3h12a*$^{-/-}$ B cells underwent a class switch in the spleen (Fig. 2a and data not shown). Furthermore, CD138^{+} CD19^{dull} plasma cells were abundant in the spleen of *Zc3h12a*$^{-/-}$ mice (Fig. 2b). In addition, the expression of CD69 was upregulated in splenic CD3^{+} T cells, and CD44^{high} CD62L^{-} T cells accumulated in the periphery (Fig. 2c and Supplementary Fig. 4a). Nevertheless, the proportion of CD4^{+} Foxp3^{+} regulatory T cells was comparable between wild-type and *Zc3h12a*$^{-/-}$ mice (Supplementary Fig. 4b). Stimulation of splenic T cells with anti-CD3 antibody resulted in increased production of IFN-γ, but not IL-17 (Fig. 2d and Supplementary Fig. 4c). Ter119^{+} (also known as Ly76^{+}) erythroblast population was higher in *Zc3h12a*$^{-/-}$ spleens, probably reflecting the responses to anaemia (Supplementary Fig. 4d). However, the ratios of B to T cells and of CD4^{+} to CD8^{+} cells were not altered in *Zc3h12a*$^{-/-}$ spleens (Supplementary Fig. 4e, f). To examine whether haematopoietic cells are sufficient for the development of disease, we transferred bone marrow cells from *Zc3h12a*$^{-/-}$ mice to recipient

[1]Laboratory of Host Defense, [2]Laboratory of Systems Immunology, WPI Immunology Frontier Research Center, [3]Research Institute for Microbial Diseases, Osaka University, 3-1 Yamada-oka, Suita, Osaka 565-0871, Japan. [4]Department of Pathology, Hyogo College of Medicine, 1-1 Mukogawa-cho, Nishinomiya, Hyogo 663-8501, Japan. [5]Research Center for Structural and Functional Proteomics, Institute for Protein Research, Osaka University, 3-2 Yamada-oka, Suita, Osaka 565-0871, Japan.
*These authors contributed equally to this work.

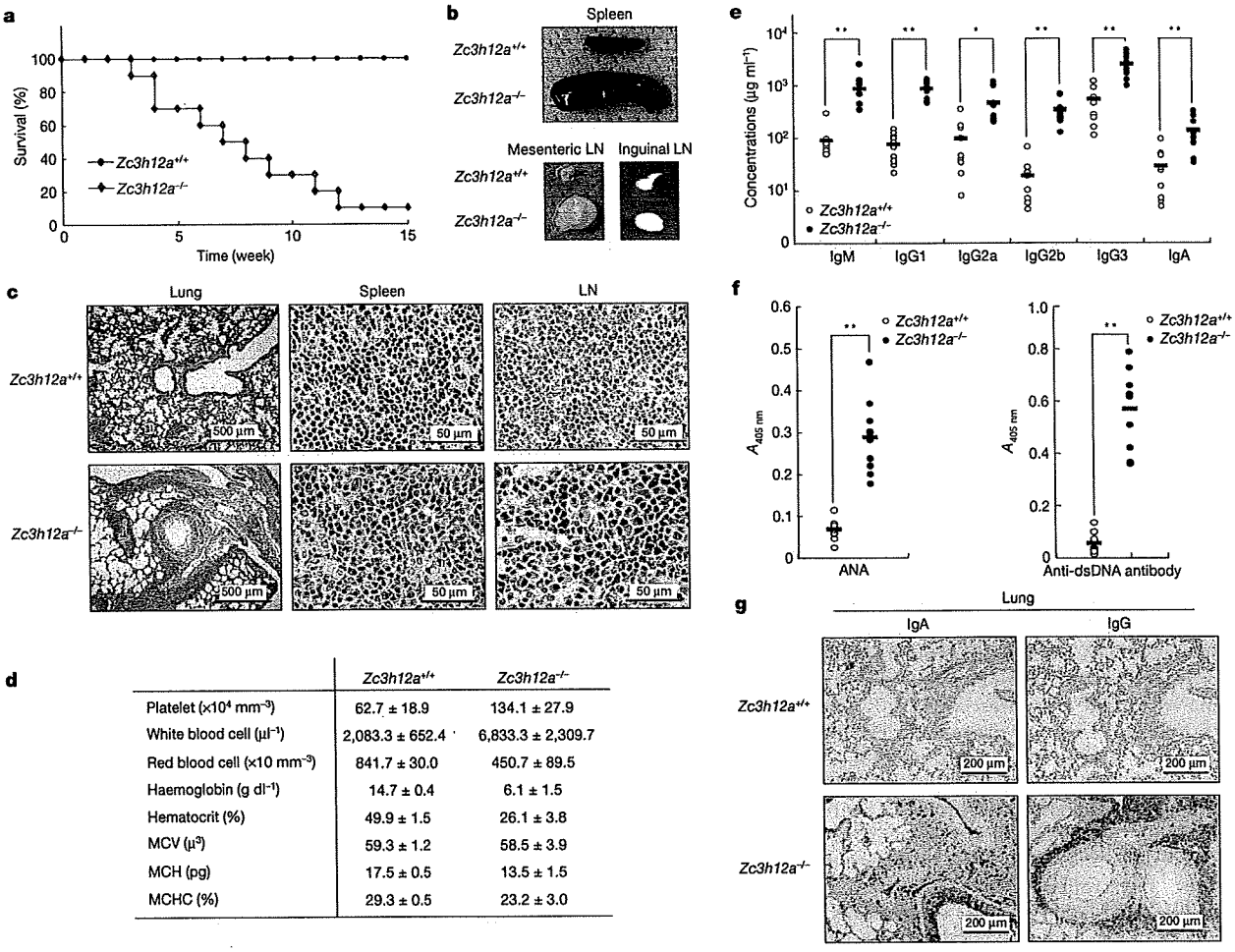

d

	Zc3h12a$^{+/+}$	*Zc3h12a*$^{-/-}$
Platelet (×10^4 mm^{-3})	62.7 ± 18.9	134.1 ± 27.9
White blood cell (μl^{-1})	2,083.3 ± 652.4	6,833.3 ± 2,309.7
Red blood cell (×10 mm^{-3})	841.7 ± 30.0	450.7 ± 89.5
Haemoglobin (g dl^{-1})	14.7 ± 0.4	6.1 ± 1.5
Hematocrit (%)	49.9 ± 1.5	26.1 ± 3.8
MCV (μ^3)	59.3 ± 1.2	58.5 ± 3.9
MCH (pg)	17.5 ± 0.5	13.5 ± 1.5
MCHC (%)	29.3 ± 0.5	23.2 ± 3.0

Figure 1 | Early onset of fetal autoimmune disease in *Zc3h12a*$^{-/-}$ mice. **a**, Survival rates of wild-type (*Zc3h12a*$^{+/+}$) and *Zc3h12a*$^{-/-}$ mice at indicated time periods ($n = 10$). **b**, Gross appearance of spleens and mesenteric and inguinal lymph nodes (LN) from wild-type and *Zc3h12a*$^{-/-}$ mice. **c**, Histology of lung, spleen and lymph nodes from wild-type and *Zc3h12a*$^{-/-}$ mice. **d**, Examination of blood cells. Data are mean ± s.d. of six samples. **e**, Hypergammaglobulinemia in *Zc3h12a*$^{-/-}$ mice. Serum immunoglobulin levels are shown. **f**, Production of anti-nuclear antibodies (ANA) and anti-double-stranded DNA (anti-dsDNA) antibodies in *Zc3h12a*$^{-/-}$ mice. Statistical significance in **e** and **f** was determined using the Student's *t*-test. $*P < 0.05$, $**P < 0.01$. **g**, Immunohistochemistry of lung sections stained with anti-IgG and anti-IgA antibodies.

C57BL/6 mice. *Zc3h12a*$^{-/-}$ bone marrow chimaeras showed delayed, but marked, development of lymphadenopathy and accumulation of plasma cells and CD44^{high}CD62L$^-$ T cells, indicating that haematopoietic cells contribute to the development of immune disorders (Supplementary Fig. 5).

Taken together, these results demonstrate that Zc3h12a is essential for preventing the development of severe immune diseases characterized by an increase in immunoglobulin-producing plasma cells and the formation of granulomas.

We then examined cytokine production from macrophages. As shown in Fig. 2e, stimulation with TLR ligands, MALP-2 (TLR2), poly(I:C) (TLR3), LPS (TLR4), R-848 (TLR7) and CpG-DNA (TLR9), induced increased production of IL-6 and IL-12p40, but not of TNF, in *Zc3h12a*$^{-/-}$ macrophages. Northern blot analysis showed that *Il6* mRNA, but not *Tnf*, *Cxcl1* or *Nfkbia* mRNA, increased significantly in response to LPS in *Zc3h12a*$^{-/-}$ macrophages, (Fig. 2f). We then performed microarray analysis to assess the difference in LPS-inducible gene expression in wild-type and *Zc3h12a*$^{-/-}$ macrophages. Microarray analysis of LPS-inducible genes in macrophages showed that most LPS-inducible genes were comparably expressed in wild-type and *Zc3h12a*$^{-/-}$ cells (Supplementary Fig. 6). Nevertheless, a particular set of genes was highly expressed in *Zc3h12a*$^{-/-}$ macrophages. These included *Il6*, *Ifng*, *Calcr* and *Sprr2d* (Fig. 2g). No differences were observed in the activation of NF-κB or the activator protein 1 (AP-1) by LPS between wild-type and *Zc3h12a*$^{-/-}$ macrophages, indicating that Zc3h12a is not involved in the regulation of the initial TLR signalling pathways (Supplementary Fig. 7).

CCCH-type zinc-finger proteins have been implicated in mRNA metabolism such as mRNA splicing, polyadenylation and the regulation of mRNA decay[4–6]. Thus, we proposed that Zc3h12a might be involved in the destabilization of mRNA, and we examined this possibility using *Il6* as an example. Wild-type and *Zc3h12a*$^{-/-}$ macrophages were stimulated with LPS for 2 h followed by actinomycin D treatment. The half-life of *Il6* mRNA, but not of *Tnf* or *Cxcl1* mRNA, increased in *Zc3h12a*$^{-/-}$ macrophages compared to wild-type cells (Fig. 3a, b). These results indicate that Zc3h12a regulates *Il6* mRNA post-transcriptionally. To determine whether Zc3h12a expression controls *Il6* mRNA, we transfected HEK293 cells stably expressing the tetracycline repressor protein fused to the transactivation domain of the viral transcription factor VP-16 (Tet-off 293 cells), with a plasmid containing the *Il6* coding sequence (CDS) with the 3′-UTR sequence under the control of a tetracycline-responsive promoter (TRE) (pTREtight-Il6-CDS + 3′-UTR). Treatment with doxycycline (dox) terminated the transcription of *Il6* mRNA, and the mRNA decayed in an incubation time-dependent manner (Fig. 3c).

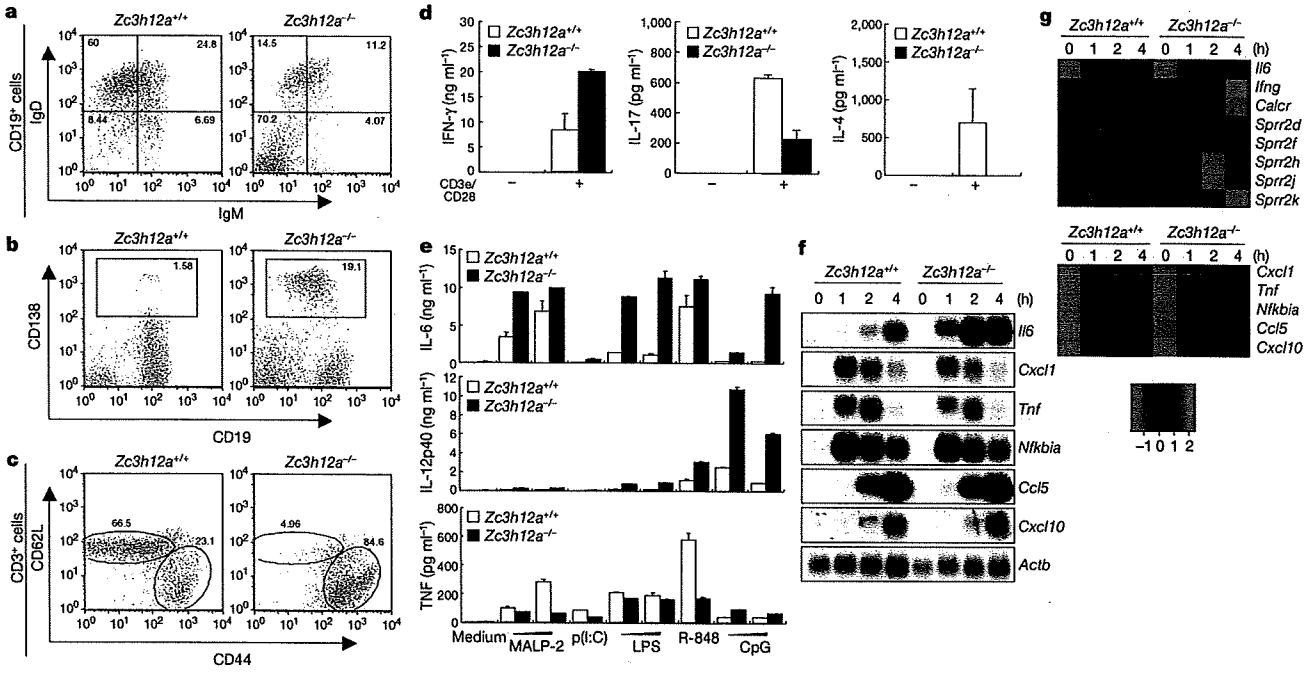

Figure 2 | Cellular abnormalities and augmented cytokine production in *Zc3h12a*$^{-/-}$ mice. a–c, Flow cytometric analysis of splenoctytes. Expression of IgM and IgD in splenic CD19^{+} B cells (**a**), the proportion of plasma cells (CD138, also known as Sdc1, and CD19) in the spleen (**b**), and expression of CD62L (also known as Sell) and CD44 in splenic T cells (**c**). Similar results were obtained in three independent experiments. **d,** Production of IFN-γ, IL-17 and IL-4 in response to CD3e and CD28 stimulation in splenic T cells. Error bars indicate s.d. of duplicates. Similar results were obtained in three independent experiments. **e,** Peritoneal macrophages from wild-type and *Zc3h12a*$^{-/-}$ mice were stimulated with MALP-2 (1, 10 ng ml^{-1}), poly(I:C) (p(I:C), 100 μg ml^{-1}), LPS (10, 100 ng ml^{-1}), R-848 (10 nM) and CpG-DNA (0.1, 1 μM) for 24 h. The concentrations of IL-6, IL-12p40 and TNF in the culture supernatants were measured by ELISAs. Error bars indicate the s.d. of duplicates. Similar results were obtained in three independent experiments. **f,** Total RNA from macrophages stimulated with LPS (100 ng ml^{-1}) for indicated periods was extracted and subjected to northern blotting for the expression of *Il6*, *Cxcl1*, *Tnf*, *Nfkbia*, *Ccl5*, *Cxcl10* and β-actin (*Actb*). **g,** Heat map representation of the expression of selected LPS-inducible genes on the basis of microarray analysis of wild-type and *Zc3h12a*$^{-/-}$ peritoneal macrophages.

Overexpression of Zc3h12a greatly accelerated the degradation of *Il6* mRNA (Fig. 3c, d). In contrast, Zc3h12a did not affect the expression of mRNA harbouring the *Il6* CDS without the 3′-UTR sequence (pTREtight-Il6-CDS) (Fig. 3c, d).

Mouse *Il6* mRNA contains five adenine-uridine-rich elements (AREs) in its 3′-UTR (Fig. 3e)[7]. In addition, a conserved element between species comprising about 30 nucleotides was reported to be important for *Il6* mRNA destabilization[8]. To investigate regions of the *Il6* 3′-UTR that are critical for conferring Zc3h12a responsiveness, we used a series of luciferase reporter constructs (pGL3) containing several regions of the *Il6* 3′-UTR (Fig. 3e). When full-length *Il6* 3′-UTR (1–403) was inserted into the reporter, the luciferase activity decreased compared to the luciferase reporter alone. Co-expression of Zc3h12a further reduced the luciferase activity of pGL3-Il6 3′-UTR (1–403) (Fig. 3f). Whereas the luciferase activities of pGL3-Il6 3′-UTR (1–70) and pGL3-Il6 3′-UTR (172–403) were not altered by the expression of Zc3h12a, the luciferase activity of pGL3-Il6 3′-UTR (56–173) decreased in the presence of Zc3h12a. *Il6* 3′-UTR (56–173) contains two AREs and the conserved element (Fig. 3f). By using a set of luciferase reporter constructs with shortened *Il6* 3′-UTRs, we found that the conserved element, but not the ARE, of *Il6* 3′-UTR was important for destabilization by Zc3h12a (Fig. 3f and Supplementary Fig. 8). Although the luciferase activity of pGL3-β-globin 3′-UTR was not affected by Zc3h12a expression, addition of the conserved element of *Il6* 3′-UTR (77–108) to β-globin 3′-UTR conferred a response to Zc3h12a (Fig. 3g). The expression of Zc3h12a reduced the luciferase activity of reporters with the 3′-UTR for *Il12p40* or calcitonin receptor (*Calcr*), but not those with the 3′-UTR of *Ifng* (Fig. 3h), indicating that *Il6*, *Il12p40* and *Calcr* mRNAs are directly regulated by Zc3h12a. IFN-γ might be secondarily regulated by the overproduction of IL-12.

We next examined whether Zc3h12a directly associates with RNA. Synthesized Zc3h12a protein, but not bovine serum albumin (BSA), associates with *Il6* 3′-UTR (1–403) RNA transcribed *in vitro*, indicating that Zc3h12a harbours an RNA-binding capacity (Fig. 4a).

Furthermore, we tested whether the CCCH sequence of Zc3h12a is critical for its role in *Il6* mRNA decay. The expression of Zc3h12a containing the C306R mutation in the CCCH zinc-finger domain, and Zc3h12a without the CCCH domain (lacking amino acids 306–322), could still destabilize *Il6* mRNA (Fig. 4b, c), although these mutant proteins had a reduced ability to degrade *Il6* mRNA when low amounts of proteins were expressed (Supplementary Fig. 9). These results indicate that the CCCH motif plays a part in the control of *Il6* mRNA decay.

The above result prompted us to look for another domain(s) responsible for mRNA decay. Sequence alignment indicated that a conserved N-terminal domain (139–297) in Zc3h12a, just preceding the zinc-finger domain (300–324), shares remote homology to the PilT N-terminus (PIN) domain-like Structural Classification of Proteins (SCOP) superfamily (Fig. 4d). Structural modelling, followed by alignment to other PIN domain structures, revealed a conserved, negatively charged pocket—formed by Asp 141, Asn 144, Asp 226, Asp 244 and Asp 248—that is potentially important for magnesium binding and enzymatic activity (Fig. 4d, e). We proposed that the N-terminal domain of the Zc3h12a protein might be an RNase, and synthesized Zc3h12a protein showed RNase activity for *Il6* 3′-UTR (1–403) mRNA in an Mg^{2+}-dependent manner (Fig. 4f, g). Zc3h12a degraded 5′- and 3′-labelled RNA with similar kinetics, suggesting that Zc3h12a has endonuclease activity (Supplementary Fig. 10). The activity of Zc3h12a seemed to be largely sequence-independent *in vitro*, because target RNAs with various sequences were degraded almost completely (data not shown). Furthermore, the Zc3h12a(D141N) mutant did not